



POLITECNICO DI TORINO
Corso di Laurea Magistrale in Ingegneria Aerospaziale
Aerospace Engineering: Propulsion Systems

Master's Degree Thesis

Static and Dynamic Topology Optimization for Aeronautical Gears



Supervisor:
Prof. Daniele Botto

Tutor:
Ing. Luca Ronchiato

Candidate:
Mariangela Casiello

December 2018

*To my pillars, GCGLL...
and to Vincenzo, who showed me the other face of love.*

Contents

| | |
|---|-----------|
| Sommario | iv |
| Abstract | v |
| Acknowledgements | vi |
| 1 Introduction | 1 |
| 2 Gears | 4 |
| 2.1 Spur Gears | 4 |
| 2.2 Helical gears | 5 |
| 2.2.1 Double helical gears | 6 |
| 2.3 Bevel Gears | 7 |
| 2.4 Hypoid Gears | 7 |
| 2.5 Worm Gears | 8 |
| 3 Optimization techniques | 10 |
| 4 Topology Optimization | 13 |
| 4.1 SIMP Method | 14 |
| 4.2 BESO Method | 16 |
| 4.3 Optimization issues | 17 |
| 4.4 Topology Optimization for an axialsymmetric structure | 17 |
| 4.4.1 Step1-GEOMETRY | 18 |
| 4.4.2 Step2-COMPONENTS DEFINITION | 18 |
| 4.4.3 Step3-PROPERTIES AND BCs DEFINITION | 18 |
| 4.4.4 Step4-LOAD STEP | 18 |
| 4.4.5 Step5-SET TOPOLOGY OPTIMIZATION PROBLEM | 19 |
| 4.4.6 Step6-POST PROCESS THE OPTIMIZED RESULTS IN HYPERVIEW | 20 |
| 5 Topology Optimization of Test Case | 23 |
| 5.1 Pre-Processing | 25 |
| 5.1.1 Defeaturing | 25 |

| | | |
|----------|--|-----------|
| 5.1.2 | DESIGN SPACE definition | 26 |
| 5.1.3 | Component Mesh | 28 |
| 5.1.4 | Model Validation | 29 |
| 5.2 | Topology Optimization process | 30 |
| 5.2.1 | Responses | 30 |
| 5.2.2 | Design variable | 31 |
| 5.2.3 | Objective function | 32 |
| 5.2.4 | Static design constraints | 32 |
| 5.2.5 | Dynamic design constraints | 35 |
| | Excitation Force | 36 |
| | Campbell Diagram | 38 |
| | FRF analysis | 43 |
| | RiskFactor calculation | 45 |
| 5.3 | Post Processing | 47 |
| 5.3.1 | Ring Test Case | 49 |
| 5.3.2 | Helical gear test case | 51 |
| | Static Optimization | 51 |
| | Dynamic Optimization | 54 |
| | Combined Topology Optimization | 57 |
| 6 | Conclusions | 61 |
| A | Modal Analysis | 62 |
| A.1 | Free vibration Systems | 63 |
| A.1.1 | Single Degree of Freedom System | 63 |
| A.1.2 | Multiple Degree of Freedom System | 65 |
| A.2 | Forced System | 67 |
| A.2.1 | Single Degree of Freedom System | 68 |
| | Velocity and Acceleration Response | 72 |
| | Force Transmission | 72 |
| | Bibliography | 74 |

Sommario

Questa tesi presenta un nuovo approccio all'ottimizzazione topologica strutturale, sono state implementate sia un'ottimizzazione di tipo statico.

Il lavoro di tesi è stato sviluppato all'interno di GE Avio S.r.l. grazie ad un accordo stipulato tra il Politecnico di Torino e GE Avio S.r.l. Lo scopo di questa collaborazione sta nello sviluppo di nuove tecnologie per i motori che equipaggeranno aerei civili futuri, e nello studio di nuovi componenti per accrescere le performance degli aerei.

Questo lavoro sviluppa una metodologia per ottimizzare il design preliminare delle geometrie degli ingranaggi per migliorare il comportamento dinamico dei componenti quindi l'obiettivo è evitare la risonanza e minimizzare l'ampiezza delle risposte agendo sul design space disponibile.

Questa tesi rappresenta l'ultimo di tre lavori di tesi volti allo sviluppo dell'ottimizzazione topologia dinamica e statica di ingranaggi. Si fa ricorso alla funzione RiskFactor la quale permette l'ottimizzazione dinamica.

Rispetto ai lavori precedenti l'ottimizzazione di tipo statico è stata analizzata in dettaglio tenendo conto del design delle dentature degli ingranaggi; inoltre, grazie all'introduzione di un numero notevole di risposte modali si riesce ad ottenere una stima realistica del comportamento dinamico in quanto si riesce ad analizzare un range di frequenze molto ampio.

È stato possibile applicare questo tool ad un ingranaggio di una gearbox in via di sviluppo, con risultati soddisfacenti.

Pertanto, la procedura matematica porta alla definizione di una risposta esterna ad Optistruct il cui output è il parametro scalare RiskFactor che conduce un'ottimizzazione strutturale come una sequenza di movimenti dei confini esterni che convergono verso una soluzione ottimale e che soddisfano i vincoli specificati.

Il risultato è una tecnica di ottimizzazione topologica per componenti tridimensionali rotanti utilizzati per la trasmissione di potenza nei sistemi di propulsione aeronautici.

Abstract

This thesis presents a new approach to structural topology optimization, dynamic and static topology optimizations have been implemented.

This MSc thesis has been carried out at GE Avio S.r.l. under a mutual industrial agreement between Politecnico di Torino and GE Avio S.r.l. The aim of this collaboration consists in developing new technologies for the next-generation civil aeronautical engines and studying new components to improve aircraft's performances.

This thesis activity develops a methodology to optimize the gear geometries during preliminary design phase in order to achieve the desired dynamic behavior of the components (avoid resonances and minimize response amplitudes) leveraging on the available design space.

This thesis represents the last of three thesis works aimed at the development of the dynamic and static topology optimization of gears. The RiskFactor function is used and it allows dynamic optimization.

Compared to previous works, static optimization has been analyzed in detail taking into account the design of the gear teeth; moreover, thanks to the introduction of a considerable number of modal responses, a realistic estimate of the dynamic behavior can be obtained as it is possible to analyze a very wide range of frequencies.

Therefore, the mathematical procedure leads to the definition of an Optistruct external response whose output is RiskFactor scalar parameter that leads a structural optimization as a sequence of motions of the external boundaries converging to an optimum solution and satisfying specified constraints.

The result is a 3D topology optimization technique for rotating components used for power transmission in aeronautical propulsion systems.

Acknowledgements

Grazie alla mia famiglia per avermi permesso di arrivare fin qui, a voi dedico questo traguardo.

Grazie a Luigi per la pazienza e il supporto durante questi 5 lunghi anni.

Grazie al mio supervisor Luca per il supporto continuo durante tutto il mio percorso e grazie al tutto il team di Gears Dynamic perchè mi ha permesso di imparare tanto e si è sempre interessato agli sviluppi del mio lavoro.

Infine, grazie a me e a quello che sono, perchè la mia determinazione e la mia testardaggine sono i termini fondamentali di questo traguardo.

List of Figures

| | | |
|-----|--|----|
| 1.1 | Engine main emissions | 1 |
| 1.2 | ACARE objectives [15] | 2 |
| 2.1 | Spur Gear | 5 |
| 2.2 | Helical Gear | 6 |
| 2.3 | Double Helical Gear | 6 |
| 2.4 | Bevel Gears | 7 |
| 2.5 | Hypoid Gear | 8 |
| 2.6 | Worm Gear | 9 |
| 3.1 | Structural Optimization | 11 |
| 3.2 | Optimization Methods [18] | 12 |
| 4.1 | The figure shows two different solutions of the same optimization problem: in particular in (a) a value of the penalty factor of 1 was imposed, while in (b) the value is 3. Note how the solution on the left does not have a defined geometry but there is only the presence of elements with intermediate density values. [4] . | 15 |
| 4.2 | the picture shows three different kinds of optimization: (a) RR=3mm, IR=10%; (b) RR=1mm, IR=0.5%; (c) RR=3mm, IR=1%. | 16 |
| 4.3 | (a) Design problem, (b) example of checkerboards, (c) solution for 600 element discretization, (d) solution for 5400 element discretization. [16] | 17 |
| 4.4 | Ring's BCs. | 19 |
| 4.5 | NO DRAW direction | 21 |
| 4.6 | SPLIT Ring's section | 21 |
| 4.7 | SINGLE Ring's section | 22 |
| 5.1 | Test case | 23 |
| 5.2 | Design process | 24 |
| 5.3 | Test case's constraints | 26 |
| 5.4 | Non Design Space | 27 |
| 5.5 | Design Space | 27 |
| 5.6 | Helical gear refined mesh | 28 |
| 5.7 | Helical gear coarse mesh | 28 |

| | | |
|------|--|----|
| 5.8 | Static Optimization Nodes | 33 |
| 5.9 | RBE3 | 33 |
| 5.10 | Static analysis results | 34 |
| 5.11 | Principle geometry parameters of gears | 36 |
| 5.12 | A-dimensionally force evolution following CR values. | 37 |
| 5.13 | Representation of oscillating force. | 38 |
| 5.14 | Adjustment factor. | 38 |
| 5.15 | Mesh frequency and natural frequencies | 40 |
| 5.16 | Forward and backward harmonics | 41 |
| 5.17 | Resonance phenomena | 41 |
| 5.18 | Comparison of Campbell diagram: fixed and rotating frame | 42 |
| 5.19 | FRF analysis results | 44 |
| 5.20 | Modal analysis nodes | 45 |
| 5.21 | Risk Factor trend | 46 |
| 5.22 | Risk Factor calculation process | 47 |
| 5.23 | Topology Optimization process | 48 |
| 5.24 | RF envelope | 49 |
| 5.25 | Ring's Campbell diagrams for each iteration | 50 |
| 5.26 | Ring model dynamic optimization | 51 |
| 5.27 | Axial-symmetrical design variable | 51 |
| 5.28 | First set up of Static Optimization | 52 |
| 5.29 | Second set up of Static Optimization | 53 |
| 5.30 | Dynamic Topology Optimization process | 54 |
| 5.31 | Engagement force profile over a period T | 55 |
| 5.32 | Frequency spectrum of the excitation force | 55 |
| 5.33 | RF envelope of Test Case | 56 |
| 5.34 | Dynamic Topology Optimization of helical gear | 57 |
| 5.35 | Intermediate iterations of Helical gear's Combined Optimization | 58 |
| 5.36 | Combined Topology Optimization of helical gear | 59 |
| 5.37 | Helical gear's Campbell diagrams for each iteration | 60 |
| A.1 | SDOF system [6] | 64 |
| A.2 | 2-DOF system. [6] | 65 |
| A.3 | Single degree-of-freedom system with viscous damping, excited in forced vibration by force acting on mass. | 68 |

| | | |
|-----|--|----|
| A.4 | Response factors for a viscous-damped single degree-of-freedom system excited in forced vibration by a force acting on the mass. The velocity response factor is shown by horizontal lines; the displacement response factor is shown by diagonal lines of positive slope; and the acceleration response factor is shown by diagonal lines of negative slope.[2] | 70 |
| A.5 | Phase angle between the response displacement and the excitation force for a single degree-of-freedom system with viscous damping, excited by a force acting on the mass of the system.[2] | 71 |
| A.6 | Response factor of a viscous-damped system | 71 |
| A.7 | Parameters of a viscous-damped system | 73 |

List of Tables

| | | |
|------|---|----|
| 4.1 | Optimization set up | 18 |
| 5.1 | Coarse mesh values shown in Fig. 5.7 | 29 |
| 5.2 | First set up of Static Optimization, Fig.5.28 | 52 |
| 5.3 | NO DRAW design card, Fig. 5.28a | 52 |
| 5.4 | SPLIT design card, Fig. 5.28b | 52 |
| 5.5 | Second set up of Static Optimization | 53 |
| 5.6 | SINGLE design card, Fig. 5.29a | 53 |
| 5.7 | SPLIT design card, Fig. 5.29b | 53 |
| 5.8 | Dynamic Optimization set up | 56 |
| 5.9 | Combined Optimization set up | 58 |
| 5.10 | Combined optimization results | 59 |

Chapter 1

Introduction

The research goal in the aeronautical field is to satisfy the demands of a constantly growing sector, offering increasingly high-quality standards and adopting sustainable solutions from an ecological and economic point of view. A continuous commitment that over the years has driven the evolution of the sector, through rapid technological advances, which have made air transport increasingly safer, more comfortable and more efficient. Today, the world of aeronautics is asking for a new and important step forward.

This thesis is part of GREAT 2020 (Great Engine for Air Traffic 2020) project which was born in 2009, promoted by the District Aerospace Piedmont Committee and co-financed by Regione Piemonte with the European Regional Development Fund. It is a research program that aims to develop innovative technologies for next-generation aircraft engines. The birth of GREAT 2020 is the crowning and natural outlet of the collaborations and relationships existing in the territory between *GE Avio Aero*, the *Politecnico di Torino* and the network of companies in Piedmont involved in the aerospace supply chain. GREAT 2020 helps to make the system structural, enhancing it and creating important synergies to sustain the different skills and abilities over time. GREAT 2020 is a great challenge, originated in Piemontese Aerospace District for the development of innovative technologies for future engines.

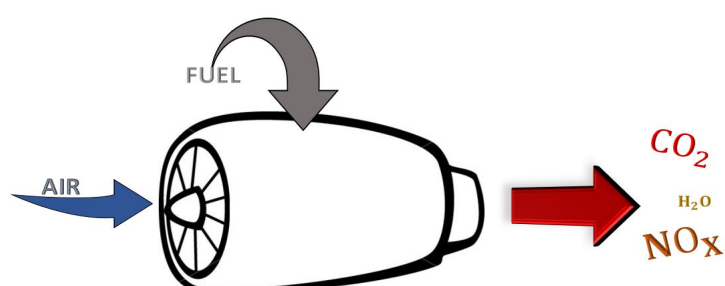


Fig. 1.1. Engine main emissions

In the aircraft engine the main emissions generated by the combustion process are carbon dioxide (CO_2) and nitrogen oxides (NO_x). If the quantity of CO_2 produced is directly proportional to the quantity of fuel burned, the formation of NO_x also depends on the thermal conditions of the combustion chamber: for example, when taking off, when the temperatures in the combustion chamber are at the highest level, NO_x emissions are maximum. Furthermore, the increase in air traffic also makes the objective of reducing the noise generated by the aircraft near airports.

The main aim of the project is to reach purposes defined by the European Commission together with a group of experts ACARE (Advisory Council for Aviation Research and Innovation in Europe), that concern 80% reduction of NO_x emission, a 50% reduction of CO_2 emission and a reduction of the perceived noise up to 10 dB in comparison with 2000 technologies as shown in Fig. 1.2.

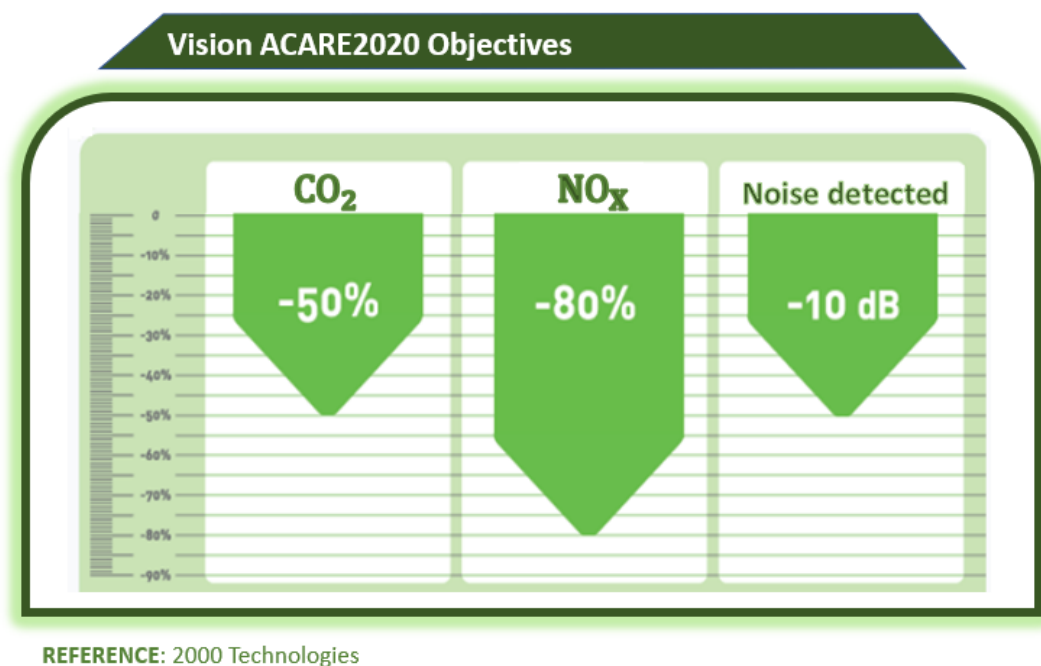


Fig. 1.2. ACARE objectives [15]

Reducing the impact of the aircraft on the environment means focusing on what is its technological heart, the engine. It provides the thrust to the aircraft and at the same time produces different types of emissions.

To reduce CO_2 emissions, it is therefore necessary to reduce the amount of fuel that must be burned to produce the necessary thrust to the aircraft; this is possible on the one hand

increasing the overall efficiency of the engine, on the other hand, reducing the weight of its sub-systems. [15]

To take part of this project the aim of this Master Thesis is to reduce the weight of a gearbox wheel starting from a defined design to increase engine efficiency.

Chapter 2

Gears

Vibration is a mechanical phenomenon whereby oscillations occur about an equilibrium point. The oscillations may be periodic, such as the motion of a pendulum or random, such as the movement of a tire on a gravel road.

Vibration can be desirable but in many cases vibration is undesirable, they may cause fatigue failure, unreliability and unwanted noise pollution, structural failure. For example, the vibrational motions of engines, electric motors, or any mechanical device in operation are typically unwanted. Such vibrations could be caused by imbalances in the rotating parts, uneven friction, or the meshing of gear teeth. Careful designs usually minimize unwanted vibrations. Vibration could be:

- **Free vibration**

This is a type of vibration in which the structure or part is disturbed and it is allowed to vibrate at its natural frequency.

- **Forced vibration**

Load, displacement or velocity are some of time-varying disturbances that could be applied to a mechanical system. The disturbance can be a periodic and steady-state input, a transient input, or a random input.

- **Damped vibration**

The vibrations are damped when the energy of a vibrating system is gradually dissipated by friction and other resistances. The vibrations gradually reduce or change in frequency or intensity.

The vibration can take place in axial, radial or tangential directions.

2.1 Spur Gears

Spur gears are the most common gears and they are used in series for large gear reductions. The teeth on spur gears are straight and are mounted in parallel on different shafts. Spur gears are used in devices as washing machines, screwdrivers, windup alarm clocks. Because of the

gear tooth engaging and colliding, spur gears are particularly loud. Each impact makes loud noises and causes vibration, which is the reason why spur gears are not used in machinery like cars. [8]

No axial thrust is created by the tooth loads. Spur gears are excellent at moderate speeds but tend to be noisy at high speeds. [10]

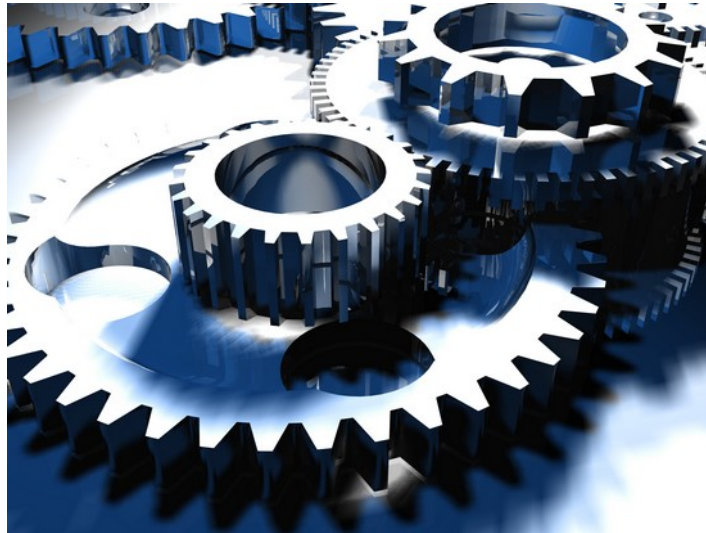


Fig. 2.1. Spur Gear

2.2 Helical gears

The helical or "dry fixed" gears are an improvement over the spur gears. The leading edges of the teeth are set at an angle with the gear rotation axis. Because of the angle the tooth shape is a segment of a helix. Helical gears can be meshed in parallel or crossed orientations. The most common orientation is when shafts are parallel to each other. Instead crossed orientation refers to non-parallel shafts, this configuration is known as "skew gears".

Helical gears operate more smoothly and quietly compared to spur gears due to the way the teeth interact. The teeth on a helical gear cut at an angle to the face of the gear. When two of the teeth start to engage, the contact is gradual-starting at one end of the tooth and maintaining contact as the gear rotates into full engagement. Helix angle can vary from 15 to 30 degrees. The thrust load varies directly with the magnitude of tangent of helix angle. Helical is the most commonly used gear in transmissions. They also generate large amounts of thrust and use bearings to help support the thrust load. [8]

The disadvantage of this solution is the production of a resulting force along the axis of the gear, which must be supported by a special ball bearing. Another disadvantage is greater friction

between the teeth caused by the increased contact surface, which must be reduced with the use of lubricants.



Fig. 2.2. Helical Gear

2.2.1 Double helical gears

Double helical gears overcome the problem of axial thrust presented by single helical gears by using a double set of teeth, slanted in opposite directions. This gear can be imagined as constituted by two distinct helical wheels placed side by side on a common axle, so that the axial forces cancel each other out. With this disposition it is possible to not use thrust bearings. Due to the complicated double helical shape these gears are more difficult to manufacture.

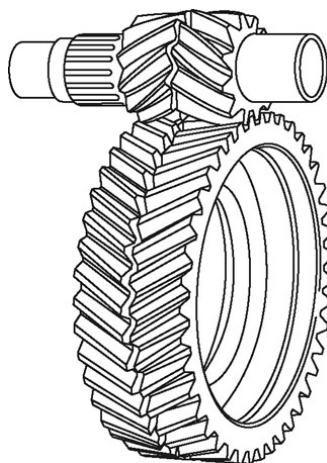


Fig. 2.3. Double Helical Gear

2.3 Bevel Gears

The Fig. 2.4 shows two different configurations for bevel gears: straight and spiral teeth.



Fig. 2.4. Bevel Gears

Bevel gears are used to change the direction of a shaft's rotation. Bevel gears have teeth that can have straight, spiral, or hypoid shape. Straight teeth have large impact when engaged in fact they have almost identical characteristics of spur gears.

Spiral teeth are like helical gear ones. They cause less vibration and noise when compared to straight teeth. The right hand of the spiral bevel is the outer half of the tooth, inclined to travel in the clockwise direction from the axial plane. The left hand of the spiral bevel travels in the counterclockwise direction. [8]

For straight and spiral bevel gears, the shafts must be perpendicular to each other and they must also be in the same plane in fact if the axis are extended they would intersect.

2.4 Hypoid Gears

The hypoid gear is composed by a larger gear called the crown and by a small gear named pinion.

The hypoid crown is a particular conical gear in which the teeth are rotated to become parallel to the rotation plane of the wheel. It meshes with a pinion with parallel or helical teeth of small dimensions.

Another variant, the hypoid conical couple, is formed by a crown and a pinion (with spiral teeth) whose axes do not lie on the same plane. For this reason, the average angle of the spiral of the crown is much lower than that of the pinion. It is quieter than bevel gears, it transmits

more mechanical moment having more overlap between the teeth of both members, it allows to reduce the height of the tunnel where the transmission shaft of the motion from the front engine to the rear deck increasing the habitability of the vehicle, while increasing the light between the ground and the differential housing.

The pinion and gear are often always opposite hand and the spiral angle of the pinion is usually larger than the angle of the gear. Hypoid gears are used in power transmissions due to their large gear ratios.[8]



Fig. 2.5. Hypoid Gear

2.5 Worm Gears

A worm gear system consists of a worm and worm wheel. The worm looks like a screw, which meshes with a worm wheel, Fig. 2.6. The worm rotates against the wheel and transfers power to the worm wheel when rotational power is applied to the former. The structure is designed so that the worm can easily turn the gear, but the gear cannot turn the worm. Some configurations expect the worm fixed in place and their designs are possible thanks to the friction between the gear and the worm.

Worm gears are the most compact type of system and provide high-ratio speed reduction. They are often the preferred kind of gearing structure when space is limited and large gear reductions are needed. Worm gears can be used to either greatly increase torque or greatly reduce speed. They are also the smoothest and quietest of the gear systems if they are properly mounted and lubricated.

Another advantage of worm gears is that they have good meshing effectiveness.

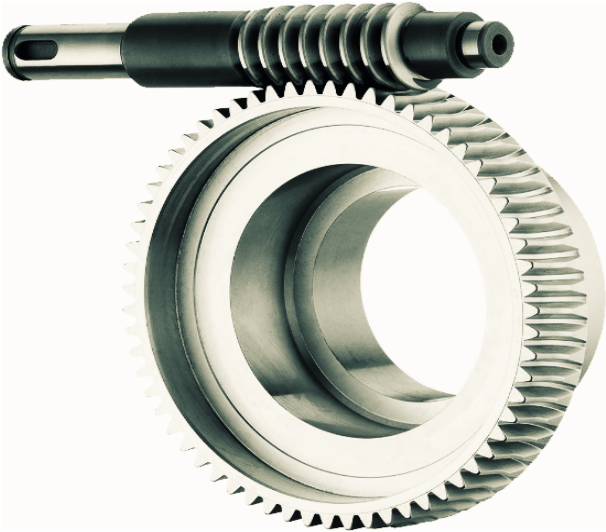


Fig. 2.6. Worm Gear

Chapter 3

Optimization techniques

There are a lot of optimization techniques and it is possible to divide them in two big parts: Shape and Size optimization and Structural optimization. First family can be divided in:

- **Shape Optimization:** to reach demanded performances, the algorithm modifies shape parameters following boundary conditions; the inputs are radius, edges, chamfers, dimensions.

Shape optimization problems employ the governing geometry variables of a shape parametrization as optimization variables, e.g. node coordinates of finite elements, control point coordinates of CAD models or morphing boxes or amplitudes of shape basis vectors.

The topology of the structure (connectivity of elements) remains constant which prevents the generation of holes.[18]

- **Size Optimization:** it is used to define structures through one-dimensional or at least two-dimensional elements; best values are calculated according to boundary conditions to reach user requested objectives. In size optimization parameters to be optimized have some geometric interpretation such as thickness, location, 1D or 2D elements properties, material properties.

Sizing optimization is used to investigate the optimal dimension of cross section parameters, which in detail are related to the applied structural model. The cross section of truss structures is defined by the cross-section area. Beam structures also carry bending loads which requires definition of more complex cross sections, e.g. by width and height or the second moment of inertia. Wall and shell structures usually define their cross section by the thickness. Due to constant model geometry and model topology differentiation of the response function with respect to sizing parameters results in facile and efficient formulations. [18]

Instead, **Structural Optimization** is composed by three kinds of analysis as shown in Fig. 3.1.

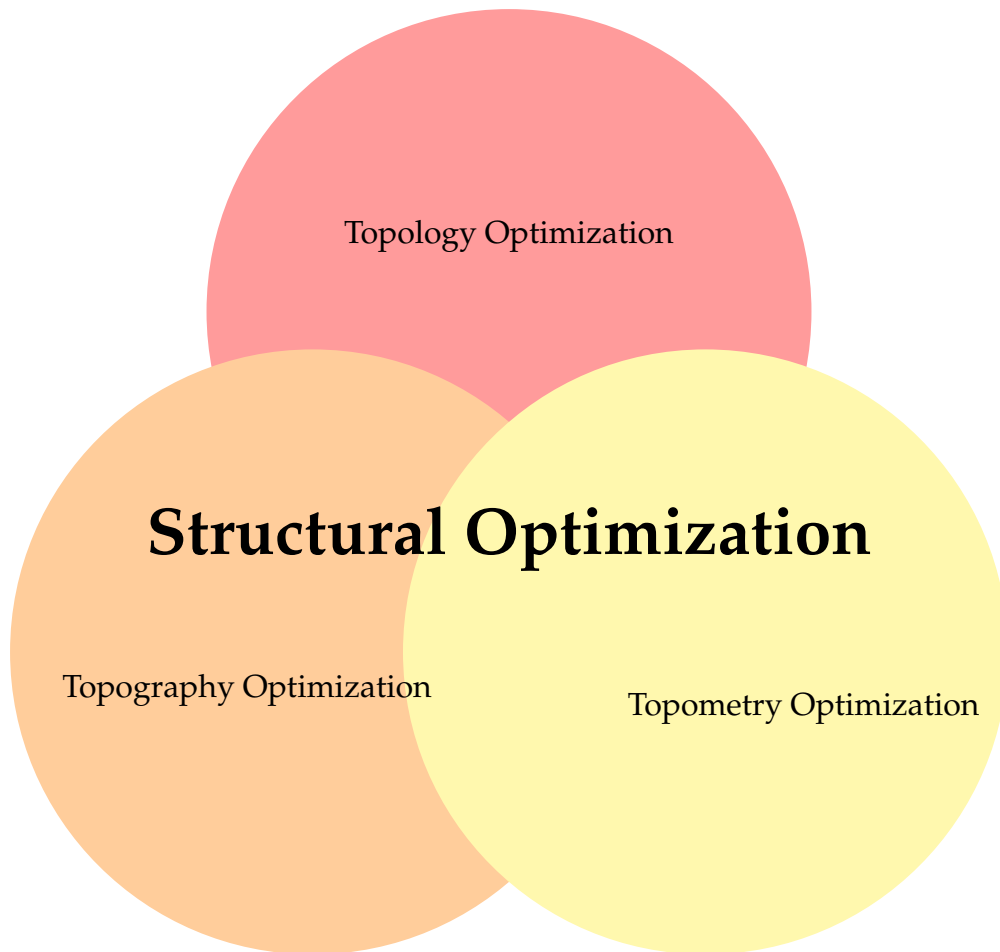


Fig. 3.1. Structural Optimization

- **Topology Optimization**
Used to define the preliminary design of components designed for the first time. The optimization method computes the most efficient material distribution in the design space respecting boundary conditions.
- **Topography Optimization**
Usually this method is used for 2D discretized elements. It calculates ribs useful to reach limiting conditions imposed by user.
- **Topometry Optimization**
It is a sort of size optimization made element by element, in fact during the process characteristics of single elements, such as thickness, 1D element properties, change to stretch out optimization objective. Instead of Topometry optimizations, Size ones employ groups of elements not just one.

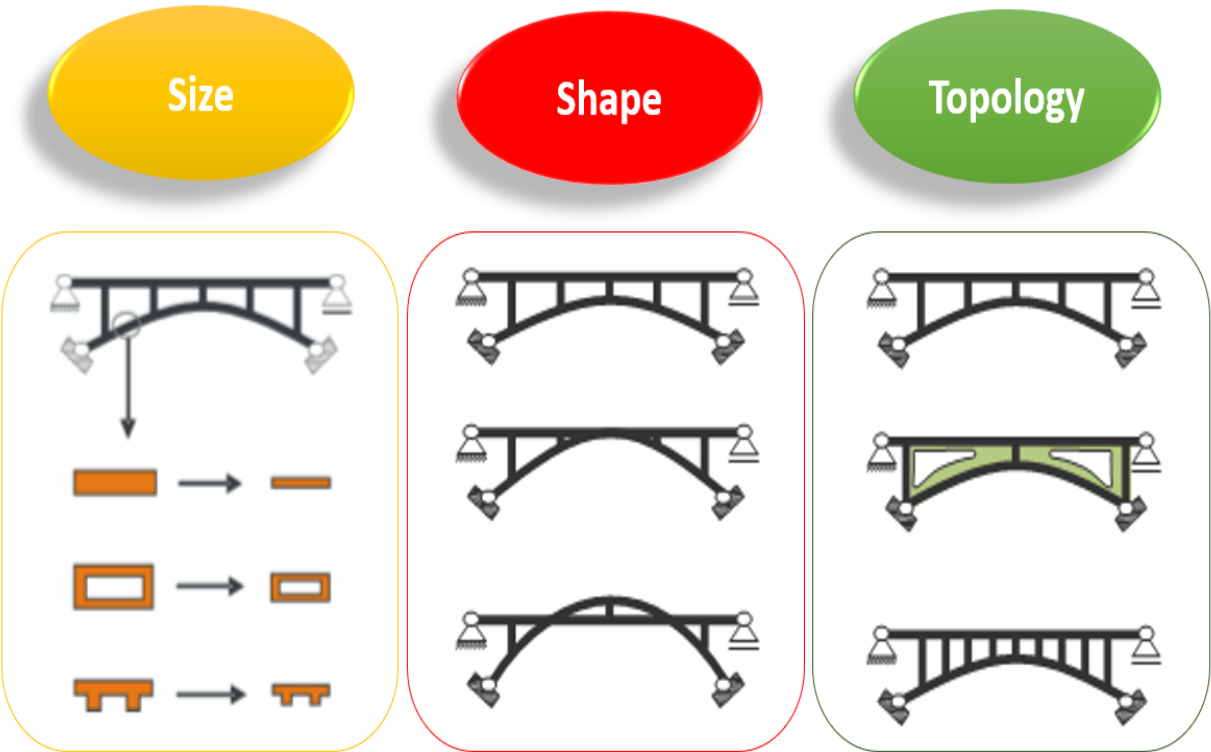


Fig. 3.2. Optimization Methods [18]

Chapter 4

Topology Optimization

One of the most difficult steps of the process is the definition of component geometry; firstly, it is defined thanks to designers' experience. This preliminary geometry is optimized through iterative methodology that involve static, dynamic and fatigue analysis which give the final part form respecting imposed design constraints.

Since dimensioning analysis are on preliminary design it is necessary to have an efficient method that give the best geometry quickly, so the technology used is the structural optimization which aims are to reduce design time and improve component performances.

Topology optimization consists on defining a geometric area and its boundary conditions, next it gives the most efficient material distribution in the design space. These optimization processes are very important not only for the preliminary design but even during redesign of components (when it is necessary to increase existent component performances.) because of the opportunity of reduced time of design and better results than those reached with traditional devices.

Topology optimization needs a generic discretized domain to perform the calculation. Before boundary conditions, material properties (Elastic module, density, Poisson coefficient) are defined. When forces and constraints are added it is necessary to define optimization parameters (maximum nodal displacement, maximum admitted tension value, first typical frequency value, etc) and at the end optimization objective which could be to minimize mass, maximize stiffness.

There are two ways of solving these optimization issues according to the calculation method used:

- **Microstructural approach:**

Problem variables are elastic material properties, which are linked to single element normalized density. The final geometry will be described by the same geometry of initial one but in this case each element has a normalized density value between zero and one. Elements with zero normalized density must be removed because they are not useful for the problem, instead elements with unitary value will describe new geometry.

There will be a lot of halfway density compared to the external values; these values are less important compared to those with unitary density value, but they could not be deleted, so it is necessary to give elements physic interpretation to evaluate their importance and the design feasibility.

There are two ways of thinking, the first one considers only elements with zero and one density values to have a clear and precise optimized geometry; the second option uses intermediate normalized density values to realize material porosity or to insert different materials.

Although, production techniques could limite advantages gained with optimization. For examples, traditional fabrication methods prevent variable density values so for those productions first way is better, alternatively additive manufacturing and lattice-optimization could realize microstructures as little as possible to manage variable density values.

- **Macrostructural approach**

Estimation variable is the component geometry therefore algorithm modifies the element dimensions and the number of elements that describe calculation domain respecting geometric constraints this means that no intermediate density values are used.

First approach is the most used since it is the most solid and it is easy to implement, it gives the possibility of anisotropic material employment. On the other hand, macrostructural approach wants well-defined starting geometry in order to have passing results; for those reasons It is usually used to optimize existing structures instead of for the new geometry design.

In literature there are so many optimization resolution methods, the most common are SIMP and BESO methods. SIMP is that used by commercial software in particular by Altair Optistruct [13] that is the one deployed in this thesis; BESO is not yet developed for calculation software. [3] [7] [14]

4.1 SIMP Method

Equations that rule topology optimization are based on energetic principles obtained by Eschenauer, Olhoff e Schnell. [13] The mathematical model with microstructural approach used in commercial software is S.I.M.P. method (Solid Isotropic Material with Penalization) that has discretized formulation with relaxation function, the process is iterative.

$$\min : F_{obj} = \sum_{i=1}^N \rho(x)^p u_i K_i u_i \quad 0 \leq \rho_i \leq 1 \quad (4.1)$$

$$E(x) = \rho(x)^p E_0 \quad p > 1 \quad (4.2)$$

Eq.4.1 explains optimization problem.

- $\rho(x)$: normalized distribution of density associated to calculation domain.
- K_i : i -th element stiffness matrix.
- F_{obj} : optimization objective function that can be maximize or minimize following the optimization's aim. In Eq. 4.1 the objective is to minimize compliance of the system.
- p : penalization factor

Eq.4.2 represents penalization function where $\rho(x)$ is linked with stiffness matrix, therefore if the density is known it is possible to give a new element stiffness value for the next iteration. The relationship between mass property and mechanicals ones has not a physical meaning but it is essential in this case.

The penalization factor “ p ” affects the solution form and worth. For a good optimization the penalization factor should be: $p > 1$ so the value assigned to the penalization factor is crucial because it can:

- Limit checkerboard issue: generation of geometry composed by zero density and unitary density elements preventing well defined geometry. These density discontinuities lead to non-linked and isolate elements which give interrupted geometry and non-feasible solution.
- Force normalized density to extreme limits (0 or 1): it avoids most of intermediate density values.

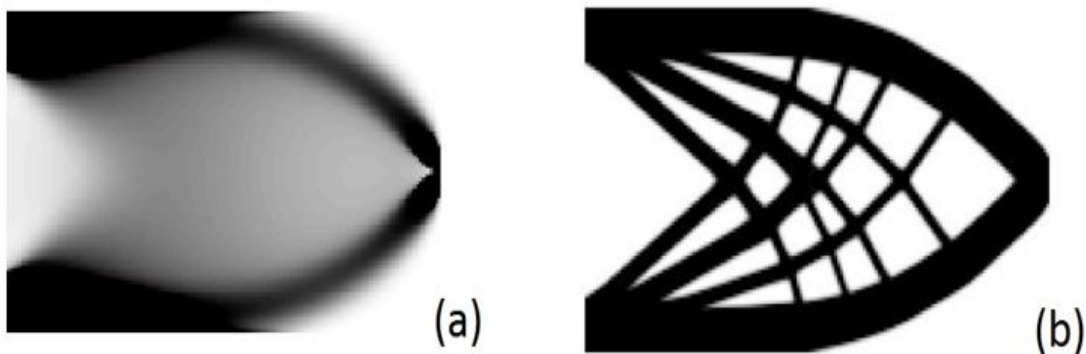


Fig. 4.1. The figure shows two different solutions of the same optimization problem: in particular in (a) a value of the penalty factor of 1 was imposed, while in (b) the value is 3. Note how the solution on the left does not have a defined geometry but there is only the presence of elements with intermediate density values. [4]

The SIMP approach could be described through next steps:

1. Calculation domain, forces and constraints definition;
2. Definition of unitary density areas, usually they are interfaces with other components;
3. Discretization of calculation domain;
4. Material properties definition;
5. Nodal displacement calculation;
6. Sensibility analysis;
7. Repetition of 5. and 6. to reach convergence;
8. Graphic representation of final density distribution.

4.2 BESO Method

Bi-directional Evolutionary Structural Optimization (BESO) aims at simultaneously adding or removing elements from the finite element model of the structure. In the ESO, because the inefficient elements are completely removed from the structure, there is no information about the effects of these elements on the objective function, in later stages of optimization. The general idea of the BESO is to devise a scheme to restore the deleted elements, if necessary. The BESO approach can be seen as a significant development that has resulted from studies on the ESO. [14]

The most important algorithm control parameters are:

- **Inclusion ratio (IR):** it indicates material variation rate during each iteration;
- **Rejection ratio (RR):** the extreme distance to calculate the sensibility index for adjacent nodes.

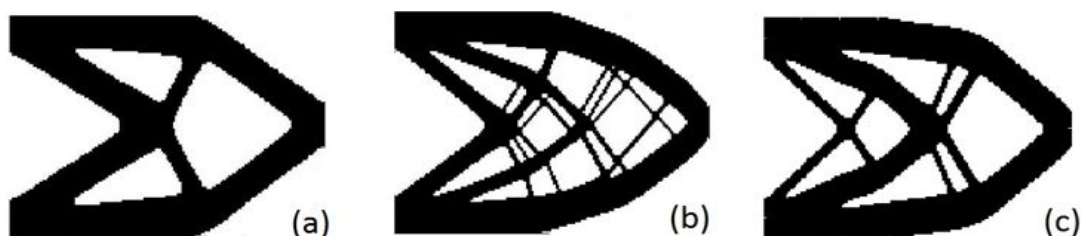


Fig. 4.2. the picture shows three different kinds of optimization: (a) RR=3mm, IR=10%; (b) RR=1mm, IR=0.5%; (c) RR=3mm, IR=1%.

4.3 Optimization issues

It is possible to divide the common numerical problems appearing in topology optimization into three categories:

- **Checkerboards** refer to the problem of formation of regions of alternating solid and void elements ordered in a checkerboard like fashion.
- **Mesh dependence** refers to the problem of not obtaining qualitatively the same solution for different mesh-sizes or discretizations.
- **Local minima** refers to the problem of obtaining different solutions to the same discretized problem when choosing different algorithmic parameters.

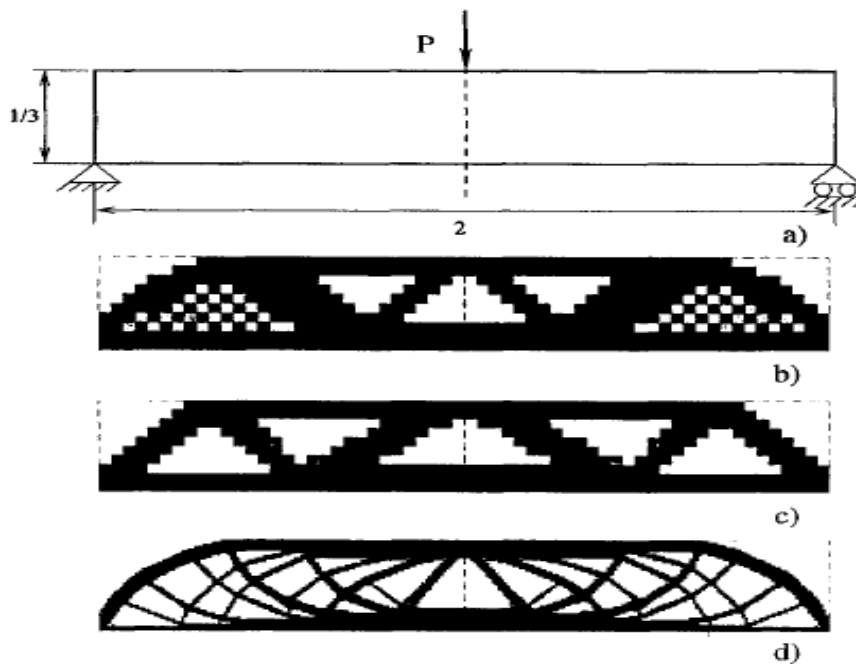


Fig. 4.3. (a) Design problem, (b) example of checkerboards, (c) solution for 600 element discretization, (d) solution for 5400 element discretization. [16]

4.4 Topology Optimization for an axialsymmetric structure

In this section we give an example of how Optistruct can be used during the Design Process. The topology optimization technique yields a new design and optimal material distribution.

Topology optimization allows designers to start with a design that already has the advantage of optimal material distribution and is ready for design fine tuning with shape or size

optimization.[12] In this section it is shown how topology is set; topology optimization is performed on a simple ring model to create a new topology for the structure, removing any unnecessary material. The resulting structure is lighter and satisfies all design constraints.

The optimization problem for this case is stated as:

TABLE 4.1: Optimization set up

| | |
|------------------|---|
| OBJECTIVE: | Minimize compliance |
| CONSTRAINTS: | Volume fraction < 0.3 |
| DESIGN VARIABLE: | The density of each element in the design space |

4.4.1 Step1-GEOMETRY

NX Parasolid has been loaded.

4.4.2 Step2-COMPONENTS DEFINITION

It is necessary to define a design space (the model part that the Optistruct must dig through iteration process respecting imposed constraints) and a non-design space (the model part that will not be modified).

4.4.3 Step3-PROPERTIES AND BCs DEFINITION

- Create material property;
- Create two PSOLID properties: DES, NON-DES;
- Assign DES to DESIGN SPACE component;
- Assign NON-DES to NON-DESIGN SPACE components;
- Create Load Collector: FORCE (it represents the contact force between two gears, it is described by three components: radial, tangential and axial);
- Select nodes and create single point constraints (SPC): this model has all DOFs constrained.

Mesh in Fig 4.4 shows the boundary conditions applied on the RING.

4.4.4 Step4-LOAD STEP

A linear static analysis of this ring structure is performed creating a static load step in which constraint and load collector are added.

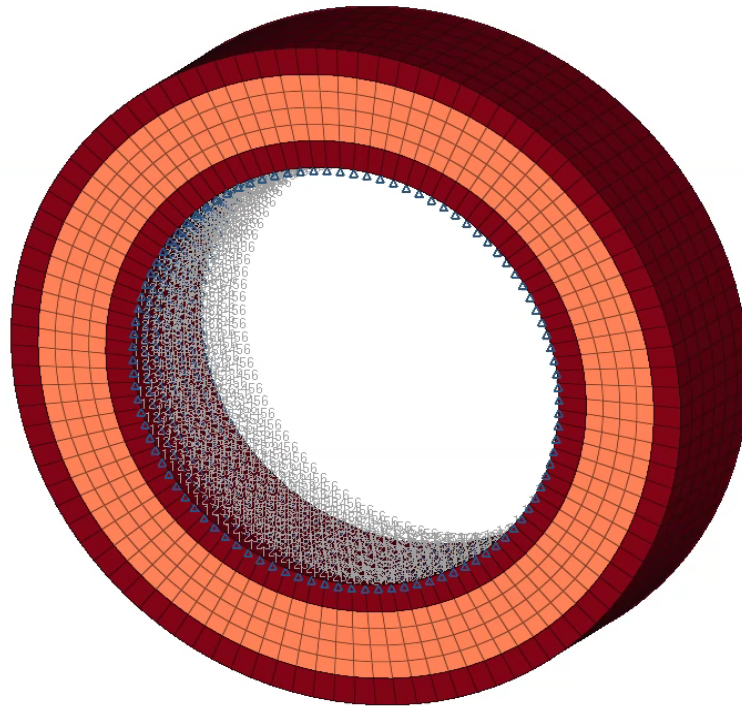


Fig. 4.4. Ring's BCs.

4.4.5 Step5-SET TOPOLOGY OPTIMIZATION PROBLEM

The finite element model, consisting of solid elements, element properties, material properties, and loads and boundary conditions has been defined. Now a topology optimization will be performed with the goal of minimizing the compliance. Typically, the material removal in an existing volume makes the model less stiff and more suitable to deformation even if it has the same loads and the same boundary conditions.

To set the Optimization problem it is necessary to:

- Define the optimization variable linking its reference property (PSOLID DESIGN PROPERTY);
 1. Settle mindim parameter to 10 ($3 * meshsize$)

That number represents a default minimum member size for use with draw direction constraints. This is determined internally to be three times the average mesh size of the relevant components. Therefore, the mesh density of the model and the target volume fraction should be chosen so that enough material is available to fill members of the default minimum size. [12]
 2. Define the pattern grouping to have a cyclo-symmetric optimization.
- Define Compliance and Volume fraction responses;

- Define Minimize Compliance as Objective, static load case is required.
- Create Constraints on Volume Fraction, the upper bound is 0.3.

The problem is completed, so we could launch the analysis. At the end of the optimization this message is shown:

```
OPTIMIZATION HAS CONVERGED.  
FEASIBLE DESIGN (ALL CONSTRAINTS SATISFIED).
```

4.4.6 Step6-POST PROCESS THE OPTIMIZED RESULTS IN HYPERVIEW

Element density and element thickness results are output from OptiStruct for all iterations. In addition, displacement and stress results are output for the first and last iteration by default. [12]

When we define the topology optimization variable during Step5, we could decide the draw direction to impose during the process. OptiStruct allows to impose draw direction constraints so that the topology determined will allow the die to slide in a given direction. Different constraints can be applied to different structural parts, specified by PSOLID IDs. There are two DRAW options available.

The 'SINGLE' option assumes that a single die will be used and it slides in the given drawing direction. The bottom surface of the considered casting part is the predefined contra part for the stamp.

The 'SPLIT' option implies that two stamps splitting apart in the given draw direction will be used to cast the part. The splitting surface of the two dies is optimized during the optimization process.

It is often requested without holes. These holes can be fend off in the direction of the draw through use of the 'NO HOLE' option. With 'NO HOLE,' the topology evolve gradually and slowly from the boundary one layer at a time, and occasionally, it may need several iterations to remove one layer.

A component may contain a non-designable region in addition to a designable region. These non-designable regions have to be defined as obstacles for the casting process. This maintains the casting feasibility of the final structure. [12]

We set 3 different analysis following this parameter:

- I) No DRAW direction: We want to see which is the final design space shape without imposed design directions.

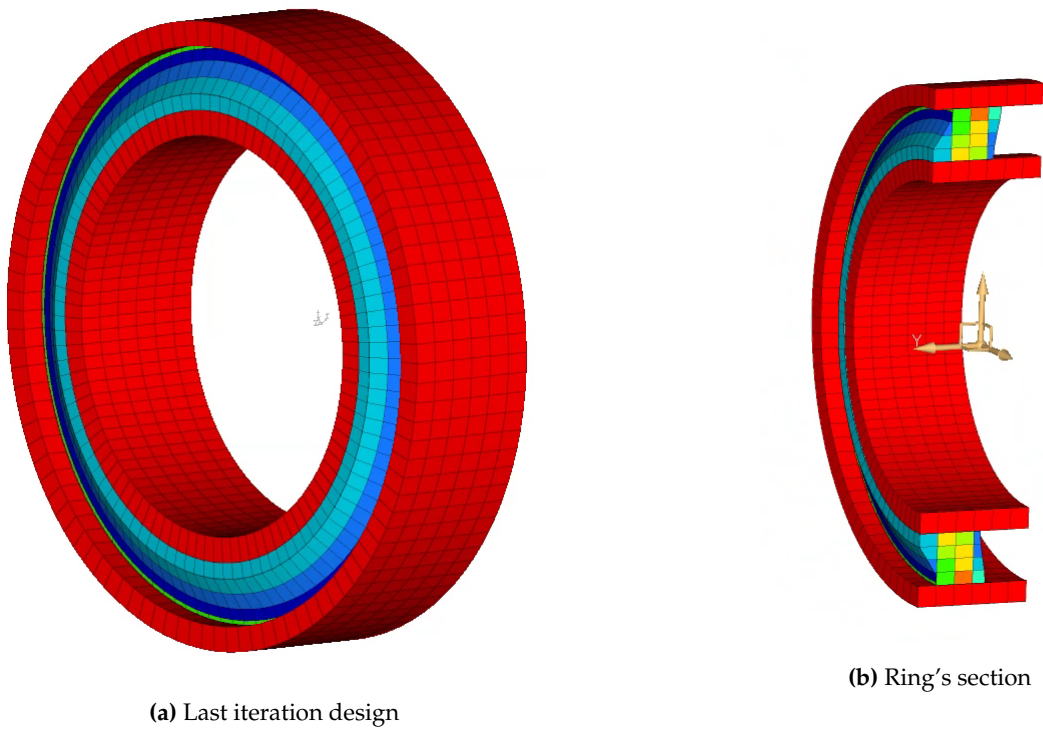


Fig. 4.5. NO DRAW direction

II) SPLIT DRAW direction

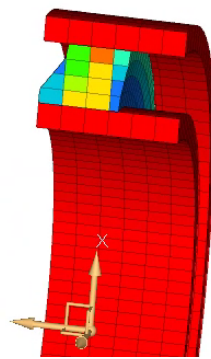


Fig. 4.6. SPLIT Ring's section

Looking at Fig. 4.5b and Fig. 4.6 we can highlight that in this case the no DRAW direction corresponds to SPLIT DRAW direction.

III) SINGLE DRAW direction

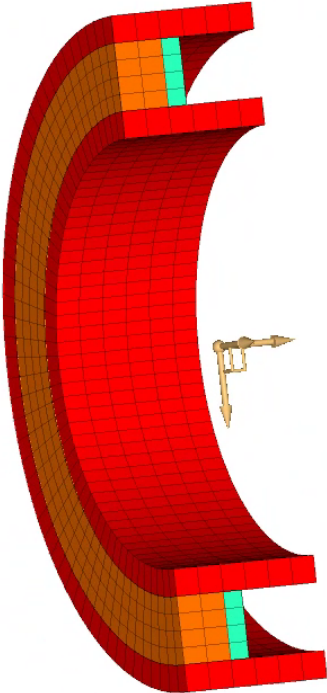


Fig. 4.7. SINGLE Ring's section

Chapter 5

Topology Optimization of Test Case

The method of Topology Optimization first appeared in the literature in 1988, and was originally developed for determining the distribution of an elastic material within an admissible design domain that subject to a given static loading yields the stiffest possible structure for a prescribed amount of material.[11]

This chapter will display the topology optimization of a helical gear which is our test case shown in Fig. 5.1.

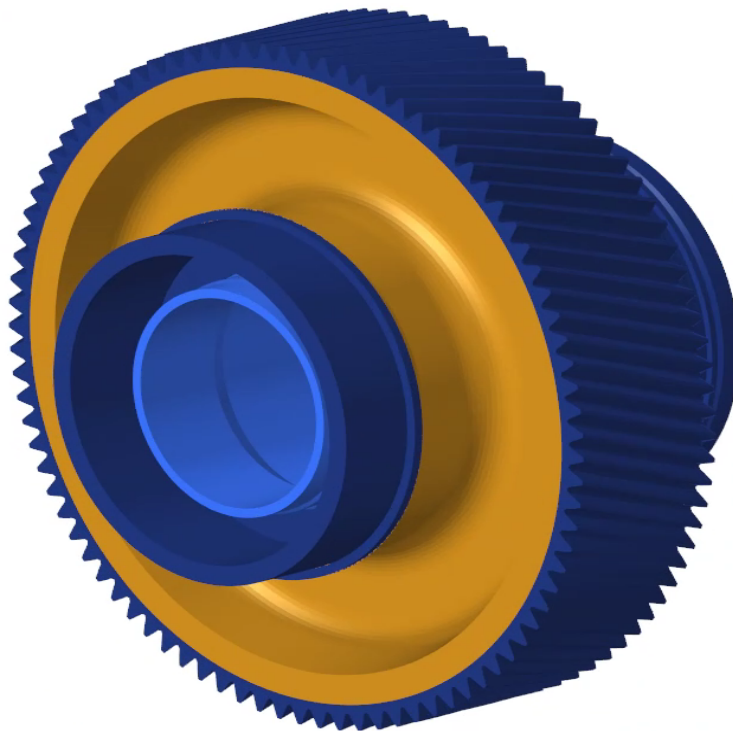


Fig. 5.1. Test case

Next flow chart, Fig 5.2, shows how design process works.

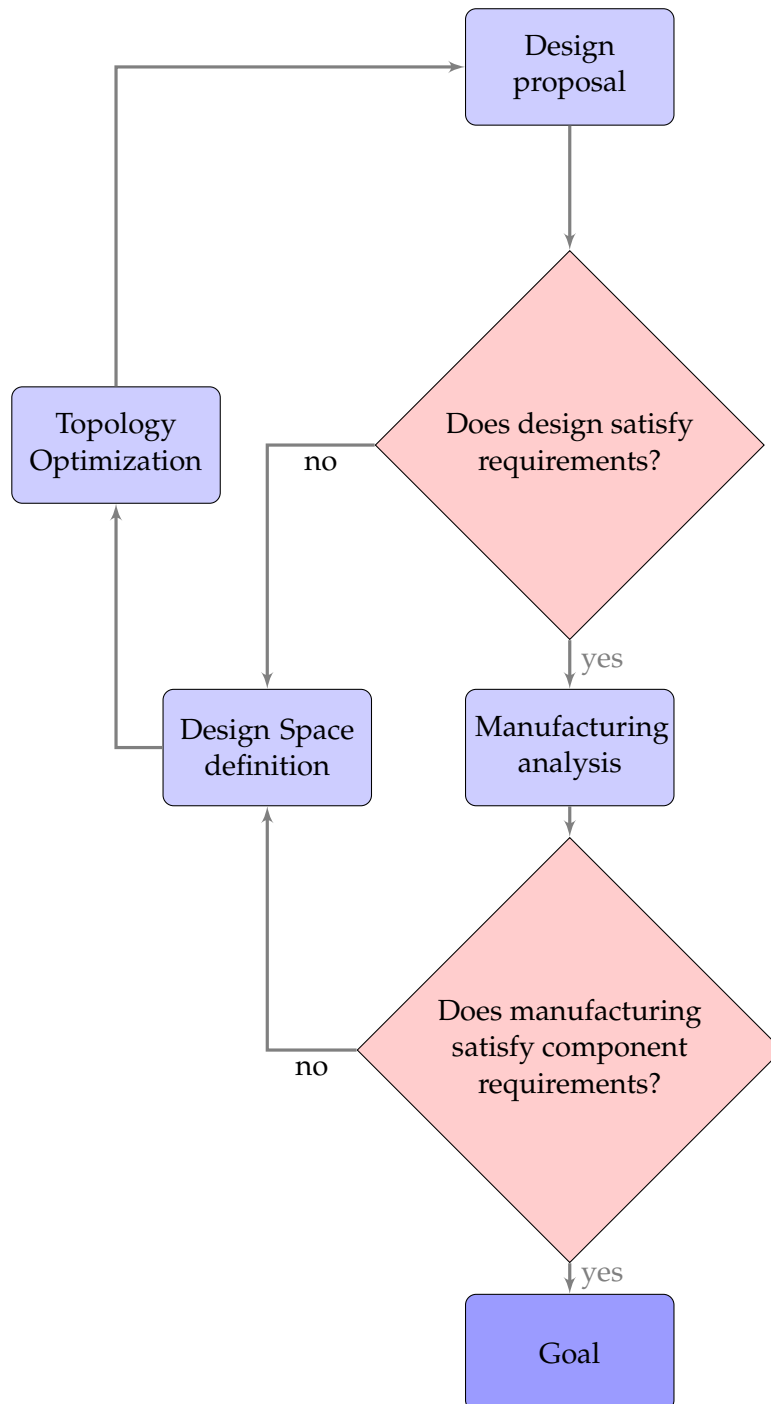


Fig. 5.2. Design process

Before starting with topological optimization, it is better to explain the problem. The problem analyzed in this thesis concerns the optimization of a helical gear. Initially, there are two versions of the same gear, the former was drawn with a slanted web but after the analyzes conducted it was discovered that this design does not fit with frequency response, so the same wheel was redesigned to get a straight and very thick web.

Gear redesign has involved a weight increase compared to first version of the wheel although the frequency response of this thick wheel is better suited to the project needs; as matter of fact if the mass goes up the vibration frequencies decrease, so it is logical that it would be better to have heavier objects with little resonance peaks in the operating range but this means having more heavier components and this consequently leads to having weighty engines which means lower performance.

The objective of this thesis work is to have a wheel that responds like the straight one but has a weight closer to that of the inclined web; with this objective, unchangeable parts like teeth, shafts, and shoulders of the bearings are defined. The set of these components is common to the two versions of the gear.

5.1 Pre-Processing

The test case analyzed in this thesis consist on a helical gear.

Pre-processing can be splitted into four different steps:

- **Defeauturing**
- **DESIGN SPACE definition**
- **Component Mesh**
- **Model validation**

5.1.1 Defeauturing

Defeauturing consists in removing all those parts of the CAD model that would be superfluous *and/or* useless in the subsequent FEM modeling and would thus involve an unnecessary waste of time and computational costs.

Therefore, we want to remove the features that do not significantly affect the behavior of the component in terms of mass, inertia and rigidity.

Defeauturing can be done both in the preliminary phase and after other operations and there are no rigid and predefined rules that require the elimination of a face or a fitting.

Defeauturing also reduces the degrees of freedom, thereby it is possible to decrease the analysis time and memory usage.

We defeature because this process gives us the possibility to increase the success ratio of mesh generation. The basic principle adopted during this procedure is that we always want to maintain, or at least do not change, the mass, inertia and overall rigidity of the structure, as these properties are the fundamental factors for the FEM analysis.

We prefer a manual approach that consists in several techniques based on the utilization of parametric deleting of features such as holes, pegs, slots, fillets, chamfers, splines in Nx environment. After each substitution we control the percentage relative volumetric difference stays under a threshold value.

At the end of this step we have the parasolid ready for HyperMesh.

5.1.2 DESIGN SPACE definition

The most important step during the setting of topology optimization is the definition of Design Space, a steel block made of selected parts which are designable during optimization process respecting the constraints imposed. Since this definition process widely influence optimization solution, we pay attention to the interfaces of the test case, the load that it must support and the structural constraints.

The gear meshes with another helical gear this is the reason why the teeth cannot be modified during the optimization process so the teeth is our upper limit. The engagement between gears leads to the contact force that will be defined in Section 5.2.4. We have thickened the teeth zone as we must take into account the thickness of the rim by following the standards for which the rim must be $1.2 * \text{tooth's height}$. We have also a lower limitation due to the shaft and to bearing shoulders.

We must define constraints (Fig 5.3), we annex two roller bearings that blocks radially, ball bearing that blocks axially, because as mentioned in the Section 2.2 the helical gear needs some bearings to balance the axial force. In addition, inside we have the spline that is bounded to the internal shaft.

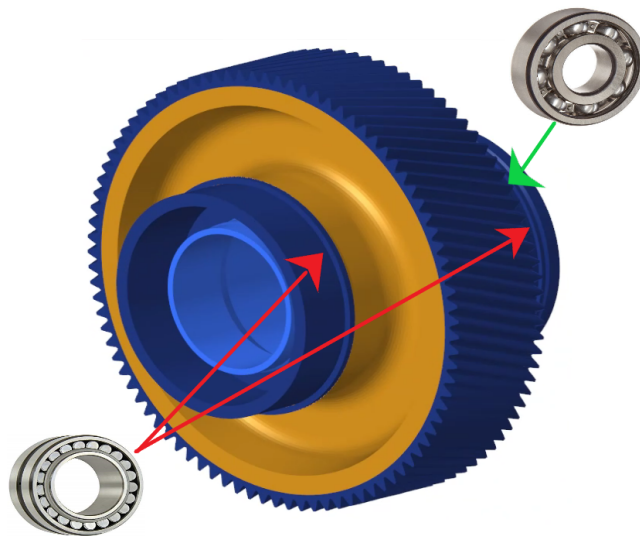


Fig. 5.3. Test case's constraints

As shown in Fig 5.4 flexible shaft, external shaft, bearing guides, teeth and rim are part of **Non Design Space**: the set of all those regions that will not change during the topology optimization.

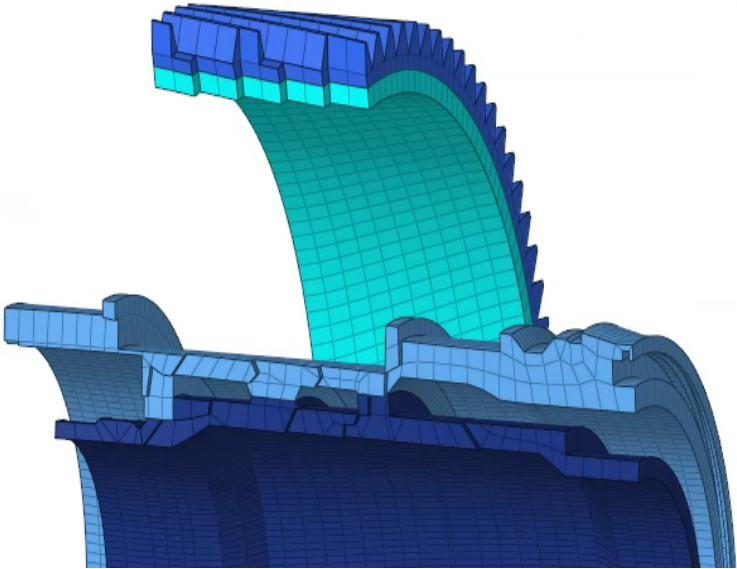
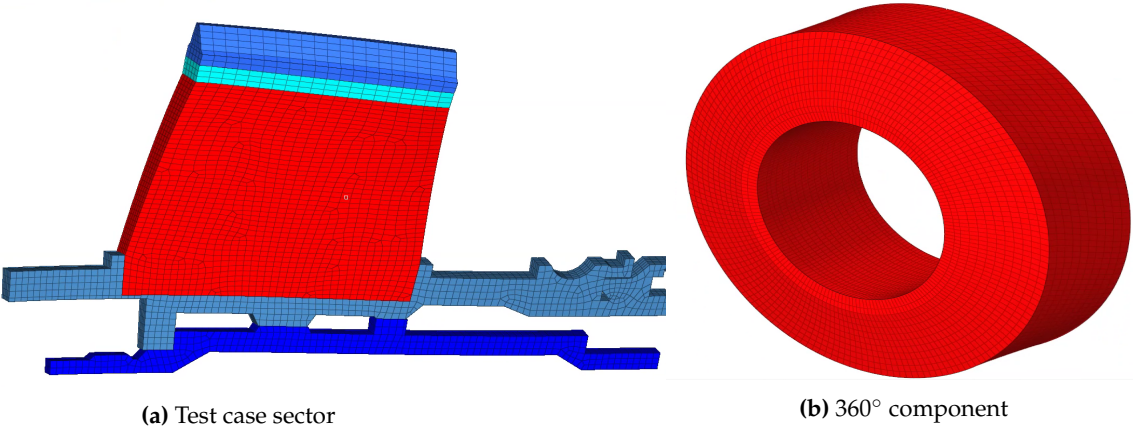


Fig. 5.4. Non Design Space

Now it is simple to see that **Design Space** will fill the empty space between teeth and shafts, as shown in Fig. 5.5.



(a) Test case sector

(b) 360° component

Fig. 5.5. Design Space

5.1.3 Component Mesh

Meshing is defined as the process of dividing the whole component into finite number of elements with their own stiffness. We choose to create two different meshes on the same component because we need a coarse mesh which makes the analysis run quickly and then gives results in a short time. Also, we created a refined mesh that allows the optimizer a much more precise work, this mesh will be used once the results from the test model become plausible, this because this definitive model will require very long analysis times.

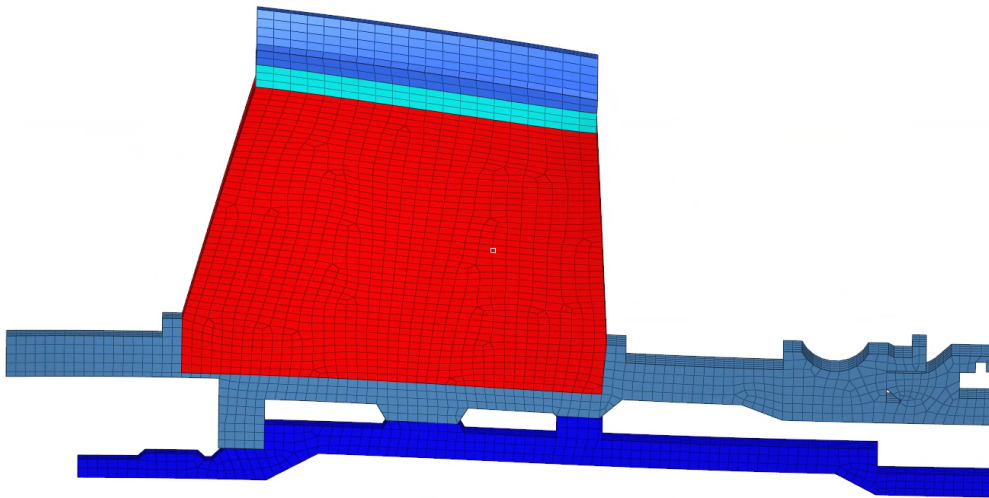


Fig. 5.6. Helical gear refined mesh

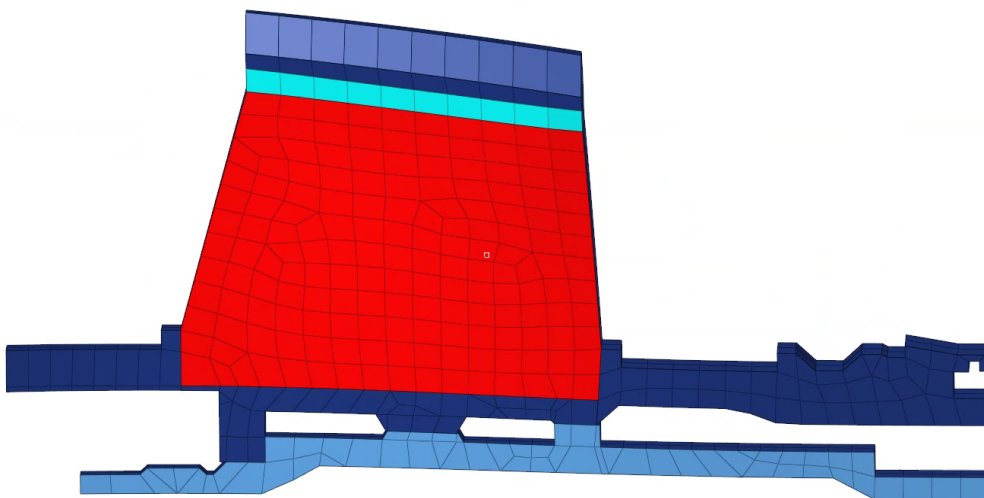


Fig. 5.7. Helical gear coarse mesh

One of the most important aspect of meshing is accuracy of the solution. It can be shown that the global solution accuracy is function of element width and the smallest vertice angle; due to this contributors it is important to check some parameters responsible for mesh quality. The meshes consist on quad elements and we check the mesh quality by examining the following parameters:

- **Warpage**

Warpage is a distortion where the surfaces of the molded part do not follow the intended shape of the design.

- **Length**

Minimum element lengths can be calculated mesuring the shortest distance from a corner node to its opposing face.

- **Jacobian**

This measures the deviation of an element from its ideal shape. The Jacobian value ranges from 0.0 to 1.0, where 1.0 represents a perfectly shaped element.

- **Chordal deviation**

Chordal deviation of an element is calculated as the largest distance between the centers of element edges and the associated surface.[12]

TABLE 5.1: Coarse mesh values shown in Fig. 5.7

| | |
|-------------------|----------|
| Warpage | > 15.000 |
| Length | > 3.000 |
| Jacobian | < 0.600 |
| Chordal deviation | > 0.100 |

9.5% of elements of the mesh shown in Fig. 5.7 fails, this mesh is acceptable for our purposes.

5.1.4 Model Validation

Before proceeding to the optimization, it was necessary to validate the model, so we performed the static, modal and FRF analysis (refear to Appendix A) on the two wheels respectively with rigid and flexible webs. To validate gear models, we compared analysis results with those reached by the designers.

To perform the analysis we have defined the contact force and the constraints as described in Section. 5.1.2.

First analysis showed different results which are due to disagreement between wheel weights, our former model does not contain the internal flexible shaft and the super-element connected with the gear through RBE2 rigid element; we will refer to this as complete model afterwards. Adding PCH we enhance mass and stiffness and in general adding mass, natural frequency rises instead adding resistance the frequency decreases, in this test case it is noted that when we add the PCH the frequency of the mode decreases so this test case is more affected by mass increase.

Taking attention to the comparison between the reference model and complete model it is possible to see that the difference in the results stands out in radial modes, this because the radial modes are sensitive to the non-design space, defined in Section 5.1.2, having defected the trees and having decreased the volume of 0.8% so we get some differences.

Once the model is validated pre-processing phase is completed. Now we are able to set the basis of topologic problem by defining the objective function, the design variable and all the design constraints.

5.2 Topology Optimization process

We start the setting of Optimization problem by defining optimization variable and a great number of structural responses.

5.2.1 Responses

Responses could be divided into:

- *Internal Responses*

Responses are defined using DRESP1 bulk data entries or by user defined function through DRESP2 bulk. DRESP2 defines responses as function of design variables, grid location, table entries, responses, and generic properties.

- *External Responses*

These responses are described by DRESP3 bulk data entry, in combination with the LOAD-LIB option entry. External responses make possible the definition of responses through user-defined external functions which may be written in HyperMath Language (HML), FORTRAN, C or a Microsoft Excel workbook. [12]

Our test case needs four kinds of Internal Responses:

1. **Static Displacement**

Displacements are the result of a linear static analysis so they need to be assigned to static load step; in particular nodal displacements can be selected as a response.

2. Volume Fraction

It consists in global response with values between 0.0 and 1.0. It describes a fraction of the initial design space in a topology optimization and take into account only the design volume. Optistruct defines volume fraction as follow:

$$\text{Volume fraction} = \frac{\text{Total volume at current iteration} - \text{Initial non design volume}}{\text{Initial design volume}}$$

3. Frequency

Natural frequencies are the result of a normal modes analysis (explained in Appendix A) hence frequency response must be assigned to the normal modes subcase.

4. Mode Shape

As frequency Mode shapes are the result of a normal modes analysis so they need normal modes loadstep. We select mode shapes as vector components.

In a structural optimization combinations of these responses can be used as:

1. Design variable
2. Objective function
3. Static design constraints
4. Dynamic design constraints

The character of a response determines whether or not a constraint or objective referencing that particular response needs to be referenced within a subcase. [12]

5.2.2 Design variable

We need to define a topology variable that means system parameter that is varied to optimize system performance. To perform a good topology optimization, it is necessary to have a little number of optimization responses, in addition for our test case we have to reduce the number of nodes and elements to run faster topology analysis. The parameters that we must take into account are the size of elements, the definition of design space by considering all the bearing loads to have a feasible design.

Since the test case is a gear we want that the latter design, that is the optimization result, would have a cyclo-symmetric shape. To achieve cyclo-symmetric shapes we can set design variable in two possible manner:

- **Extrusion constraints :**

This option enables to obtain a constant cross section along a given path, particularly in

the case of parts manufactured through an extrusion process. By using extrusion manufacturing constraints in topology optimization, constant cross-section designs can be obtained for solid models regardless of the initial mesh, boundary conditions, or loads.

- **Cyclic pattern grouping:**

The cyclical pattern grouping allows to force Optistruct to create a series of symmetric shape variables about a central axis that repeat a number of times determined by user thanks to the UCYC field.

5.2.3 Objective function

Objective function is represented by any response function of the system to be optimized. The response is a function of the design variables. Our Topology Optimization objective function is **Static Compliance** that physically this can be interpreted as a measure of strain energy in the structure:

$$C = \frac{1}{2} \int \epsilon^T \sigma dv = \frac{1}{2} U^T F = \frac{1}{2} U^T K U \quad (5.1)$$

In a case with prescribed load (F), a structure is said to be stiffer when the displacement (U) is low, thus making minimizing compliance equivalent to maximizing stiffness; instead, when prescribed displacement is considered, a structure is considered stiffer if the force to achieve that displacement is high, thus maximizing compliance corresponds to maximizing stiffness. Prescribed loads is used in this project, this means that a lower compliance means a stiffer structure. As stated before, C can be considered a reciprocal measure of the stiffness (K):

$$C = \frac{1}{2} U^T F = \frac{1}{2} \frac{F^T F}{K^T} = \frac{1}{2} \frac{f^2}{K} \quad (5.2)$$

where $\frac{1}{2} f^2 = constant$.

Last step of this topology optimization is inherent in constraints' definition, it necessary to define bounds on system response functions that need to be satisfied for the design to be acceptable.

5.2.4 Static design constraints

To perform Static Topology Optimization we use static displacement described in Section. 5.2.1. To conduct static optimization it is necessary to define a static subcase that refers to the defined constraints and to the contact force whose formulation is expressed in Eq.5.3.

The contact force has three components: tangent, radial, axial forces; for helical gear meshing

force components are:

$$\begin{cases} F_T = \frac{T}{r_m} \\ F_R = F_T \frac{\tan(\phi_n)}{\cos(\psi)} \\ F_A = F_T \tan(\psi) \end{cases} \quad (5.3)$$

In this test case we have defined the static by referring only to the shifts of the nodes on the root of the tooth, that are those border nodes between the tooth and the rim.

We decided to consider 6 nodes, 3 on one side of the toothing and 3 on the other side as shown in the Fig. 5.8. These 6 nodes are not positioned at random but have been taken around the tooth on which the force, indicated in red, is applied.

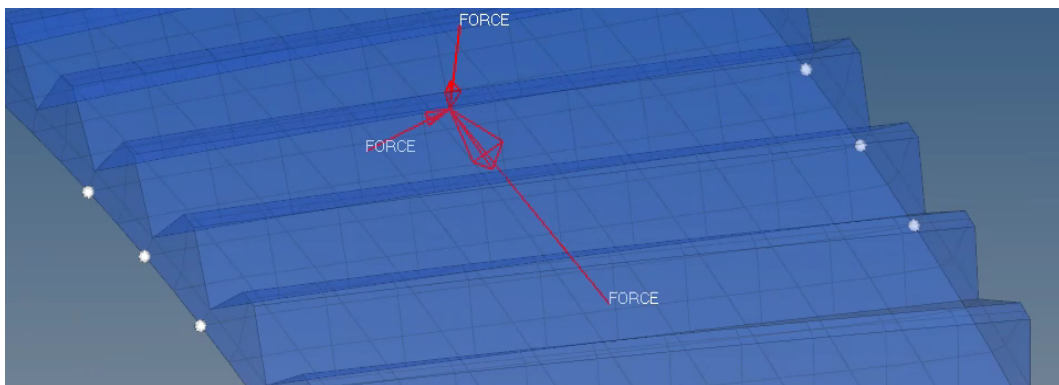


Fig. 5.8. Static Optimization Nodes

First approach to static definition was to define a RBE3 that connected all the nodes indicated, Fig. 5.9, by this way we would have to also constrain the degrees of rotational freedom, but to limit the number of optimization responses we decided to define the static based on the 6 nodes, and so we have to constrain the translational degrees of freedom. The solid elements do not have rotational degrees of freedom that we find instead in the static elements like the RBE3.

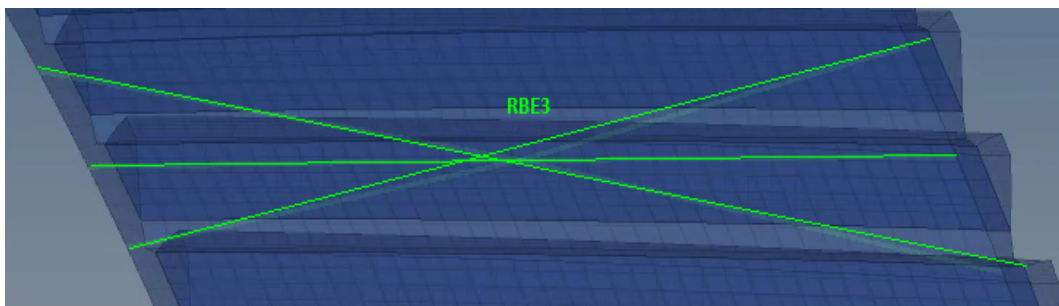


Fig. 5.9. RBE3

For each node we define X_R, X_T, X_Z , which are the radial, tangential and axial static displacements which correspond to DRESP1 responses.

After defining these answers, thanks to DRESP2 bulk we make the average of the displacements of the 6 nodes in the three directions to define the static optimization setting, Eq.5.4.

$$\begin{cases} R = \frac{1}{6} \sum_{i=1}^6 X_{R_i} < R_{lim} \\ T = \frac{1}{6} \sum_{i=1}^6 X_{T_i} < T_{lim} \\ A = \frac{1}{6} \sum_{i=1}^6 X_{Z_i} < Z_{lim} \end{cases} \quad (5.4)$$

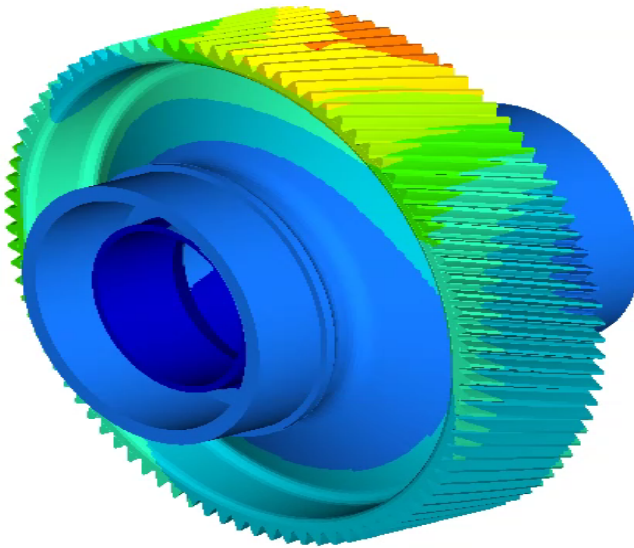


Fig. 5.10. Static analysis results

Values use to constrain the average displacements in the three directions (R,T,A defined in Eq. 5.4), we refer to the results of static analysis of the flexible web gear, Fig. 5.10 and multiply them by a multiplicative coefficient.

We are not very conservative since the displacements of the flexible gear are much larger compared to those of the rigid gear but we can operate great modifications on the tothing, so we can use this kind of results.

Once both static topology and objective function (Sec. 5.2.3) are defined we have to consider one more design constraint referred to *Volume Fraction*. As reported in Sec. 5.2.1 it is an internal response with values between 0.0 and 1.0.

Since we want to drastically reduce the volume and consequently the weight of the optimized component to reach a weight like that of flexible web gear we calculate the limit as follow:

$$\% \text{ of } V_{FRAC} = \frac{V_{DES SPACE} - V_{FLEXIBLE WEB}}{V_{DES SPACE}} = 26\% \quad (5.5)$$

So we use as upper limit to constrain Volume Fraction:

$$V_{FRAC} = 0.3 \quad (5.6)$$

By defining previous design constraints and objective function we set Static Topology Optimization which results will be shown in Sec. 5.3.

Now we will define the Dynamic part of the optimization.

5.2.5 Dynamic design constraints

Since the dynamic behavior of aeronautical gears is extremely complex and strict to be included in a commercial software like Optistruct, it is necessary to implement a custom response and to develop a script that can collect all the dynamical parameters required to define a design constraint useful for the optimization.

How explained in Sec. 5.2.1 it is possible to define external responses through DRESP3 bulk data in Optistruct environment.

The process referred to in this section was previously started by Carlo Artero in 2018 [1] which is based on the previous work by Luca D'Alò [5].

The aim of this thesis is to generalize previous models and to validate them, our test case concerns about helical gear.

D'Alò after observing the characteristics of the dynamics of the gears has defined a parameter called **Risk Factor** that summarizes gears' dynamic behavior.

The risk factor represents an index of the level of danger of the frequency response of a gear excited by an external force.

We want to avoid resonance peaks or at least reduce them amplitudes in all engine operative conditions such as Takeoff, Idle, Cruise and Landing.

RiskFactor definition considers:

1. *Peaks of resonance amplitude*

Maximum risk is assigned to all peaks greater than a threshold value and the other will be rescaled between 0 and 1 after a linear normalization.

2. *Peaks of resonance distance from operative conditions*

Maximum risk is assigned if the peak is close to an operative range (OR) and linearly decrease to zero when it is out of a margin range.

3. *Load applied in each operative condition*

Risk is rescaled using torque value of each OR, to give more importance to peaks situated at higher RPM.

4. *Total number of peaks inside the Operative Range*

Risk increases with the number of total peaks present in the RPM range between the minimum and maximum operative speed.

We define a great number of modal shapes and natural frequencies responses and we link them together through DRESP3 external response in Optistruct and we pass it as input to HML

script written in HyperMath language. During each iteration of the topology we extract Risk-Factor value and we constrain this output by assigning a threshold that represents the best dynamic behavior.

To validate this optimization process we define the:

- Excitation Force
- Campbell diagram
- FRF analysis
- RiskFactor calculation
- Ring Test Case

Excitation Force

Excitation force is the oscillating part of the contact force and it is estimated as a percentage of the total force. The dynamic force's percentage used to excite gears to have gears' frequency response, changes following harmonic order. In this thesis excitation force is represented by the meshing force developed between the teeth profiles of two gears and it is applied to pitch diameter.

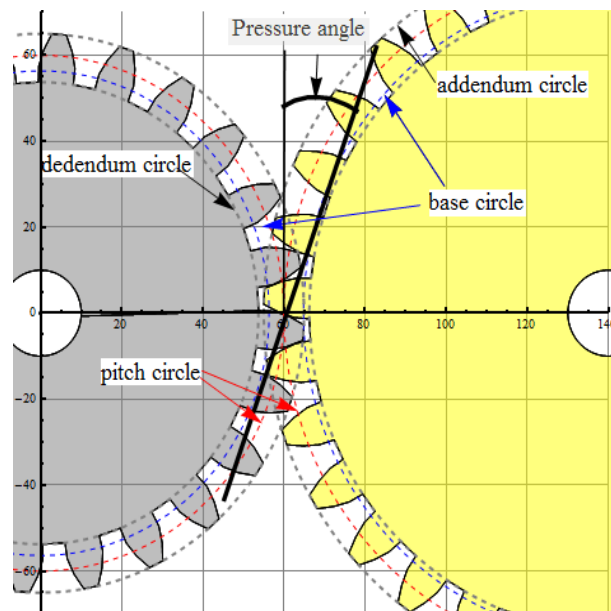


Fig. 5.11. Principle geometry parameters of gears

More fitting force values may be reached thanks to the *Fast Fourier Transform*, FFT gives the force value in harmonic domain. As a consequence, force is described by phase and amplitude. Approximation of the force can be represented by a trapezoidal shape whose height is determined by static force amplitude and by Contact Ratio value. The Contact Ratio (CR) is a value which represents the average number of teeth engaged.

- $CR = 1$ represents an ideal condition and for that value the shape of the trapezoidal degenerate in a rectangle.
- $1 < CR < 2$ means that the force shape will be a trapezoidal whose height reach the maximum force value. \rightarrow *straight tooth gear*
- $CR = 2$ the trapezoidal force shape degenerate into a triangle, in this case a single tooth must handle all the load on his own.
- $CR > 2$ the trapezoidal height will never reach the maximum value of force because there are more than two teeth engaged during gear meshing. \rightarrow *helical gear*

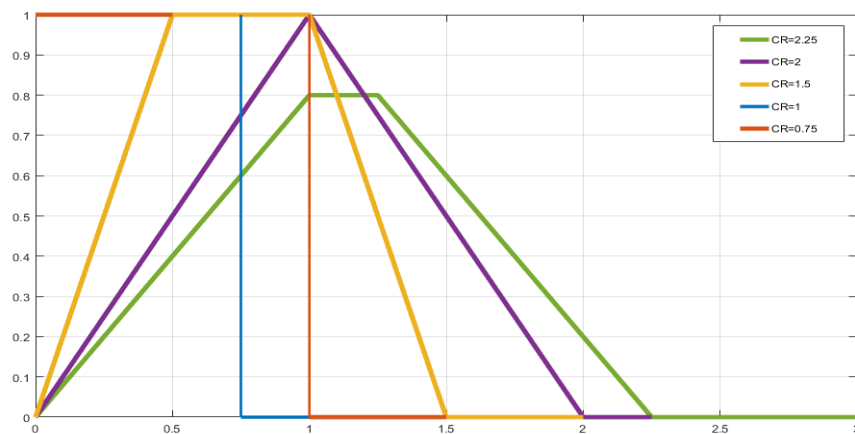


Fig. 5.12. A-dimensionally force evolution following CR values.

We need another parameter to correctly evaluate the excitation force: the adjustment factor that must be multiplied for the static force to obtain the correct excitation value.

Supposing that the force has trapezoidal shape but in addition excitation force would have fluctuations around the mean value of the force. The adjustment factor K_v summarize these fluctuations.

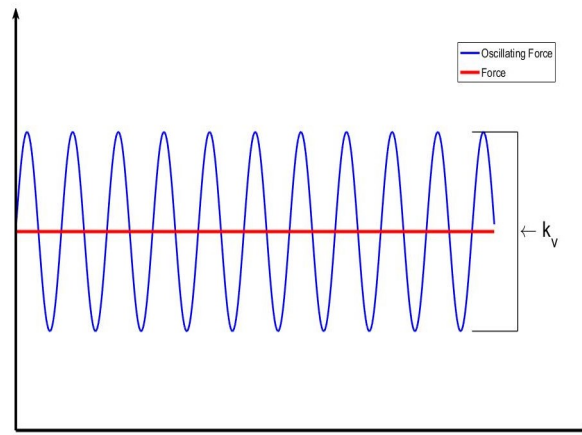


Fig. 5.13. Representation of oscillating force.

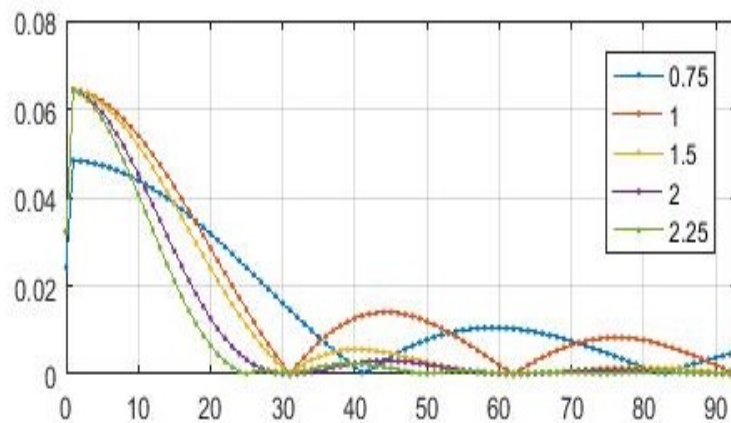


Fig. 5.14. Adjustment factor.

K_v can assume values shown in Fig.5.14 and in our analysis we choose $K_v = 1$ since we do not consider the fluctuations.

Campbell Diagram

Dynamic behavior of gear systems is important for two main reasons. One reason is the durability of the gear pair. Forces acting at the gear meshes and bearings under dynamic conditions might be many times larger than corresponding quasi-static forces. As a result of this, stresses, and hence, bending and contact fatigue lives of a gear set are influenced by its vibratory behavior, that is the reason why gears' design standards incorporate a dynamic rating factor in

an attempt to account for such dynamic effects. The second reason that makes the dynamic behavior relevant is the noise generated by the gear set. Time-varying dynamic gear mesh and bearing forces are transmitted to surrounding structures through the housing and the mounts to cause gear whine noise. Therefore, large vibration amplitudes typically result in higher noise levels as well.[17]

How described in Appendix A mechanical system' properties can be described by Stiffness (**K**), Mass (**M**) and Damping (**C**). Mass and stiffness properties determine structure's natural frequencies and mode shapes; on the other hand, damping determine the amplitude of the vibration response.

Unlike static analysis, performed with neither mass nor damping contributions, dynamics are mainly concerned with studying the frequencies of these forces in order to design gears systems by avoiding resonances in operative range.

Modal shape is defined by a number of zero displacement areas called *nodal diameter*, it is also possible to have diametric circumferences. When subjected to an excitation force, pairs of nodal diameter modes combine to form a single sinusoidal wave with any circumferential orientation. Thus, the cosine and sine modes are not distinguishable in an experimental set-up.

Modal analysis returns double modes which mean having two modes at the same frequency but with different orientation of the nodal diameters and therefore of the different modal shape.

Hertzian contact, body deflection, profile modifications such as tolerances and design issues make the contact between teeth not perfect and this leads to the definition of *Transmission Error*. In geared systems, the Transmission Error is defined as the difference between the angular position of the wheel and the position it would have had if the transmission been perfect (infinite stiffness and perfectly conjugated teeth) with reference to the pinion position. [9]

We have that at zero speed if we hit the gear, it begins to vibrate at its own natural frequencies, they are represented in Fig 5.15 by circle on frequency axis.

As a component rotate it emits a vibration response at a certain amplitude. As the speed of rotation changes, the response changes. Engine order (n) tracks the relationship between this response, the RPM and the frequency of the rotation.

$$f_i = \frac{n * \Omega}{60} \quad (5.7)$$

Then increasing the speed, the point of contact moves, its motion is periodic because the contact is repeated after a certain period then the contact force is represented by a harmonica. The frequency at which contacts happen depends on the operating speeds (Ω), number of teeth (Z) and Engine Order (n) and it is called *mesh frequency*:

$$f_{MESH} = n * Z * \Omega [Hz] \quad (5.8)$$

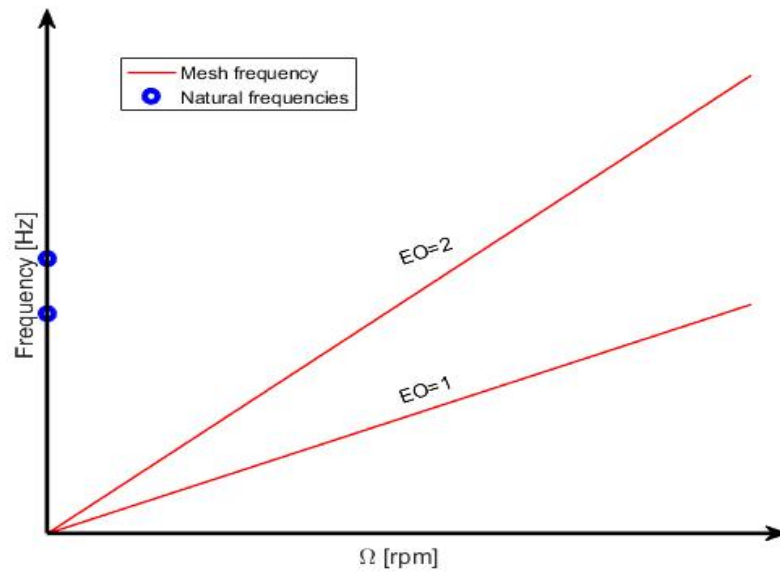


Fig. 5.15. Mesh frequency and natural frequencies

Since gears vibrate while rotating, it happens that two harmonics waves are contributing to dynamics. Therefore, depending on whether these harmonics have the same sign or not, the natural frequencies change with the speed. In a Campbell diagram, this is represented by two lines starting from the natural frequency, shown in Fig.5.16 on the vertical axis. The aperture between these two lines follows the law:

$$f_i = f_0 \pm slope\Omega \quad (5.9)$$

Where:

- f_0 represents the natural frequency at zero speed
- Ω is the rotating speed
- *slope* could be divided into:
 1. Radial slope: $N_D \frac{N_D^2 - 1}{N_D^2 + 1}$
 2. Axial slope: N_D
- N_D stands for the nodal diameter's numbers

Eq.5.9 is well founded if there are not gyroscopic effects and forward and in addition backward harmonics are symmetric, Eq. 5.9 leads to the definition of:

- **Forward harmonic:** The mode shape will rotate in the same direction of the gear. The harmonica of the contact and the natural one turn in the same verse, they are added together.

- **Backward harmonic:** The mode shape will rotate in the opposite direction of the gear. The harmonica of the contact and the natural one are subtracted.

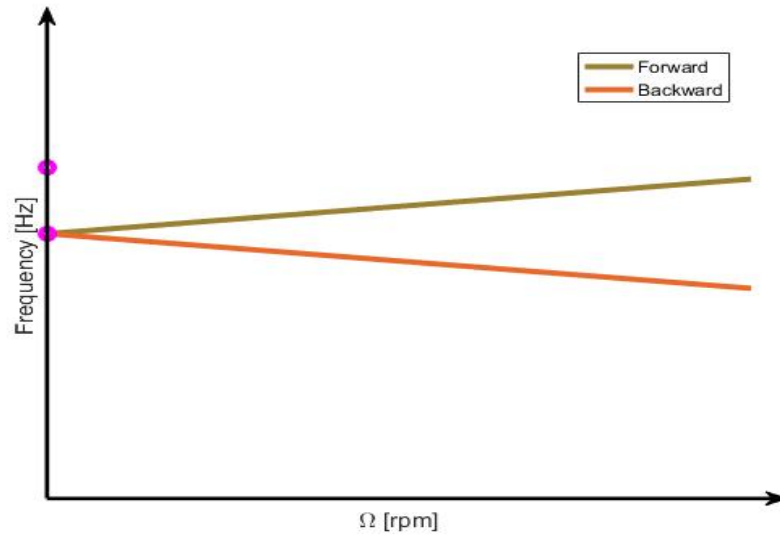


Fig. 5.16. Forward and backward harmonics

When forward and backward harmonics intersect the mesh frequency, resonance happens.

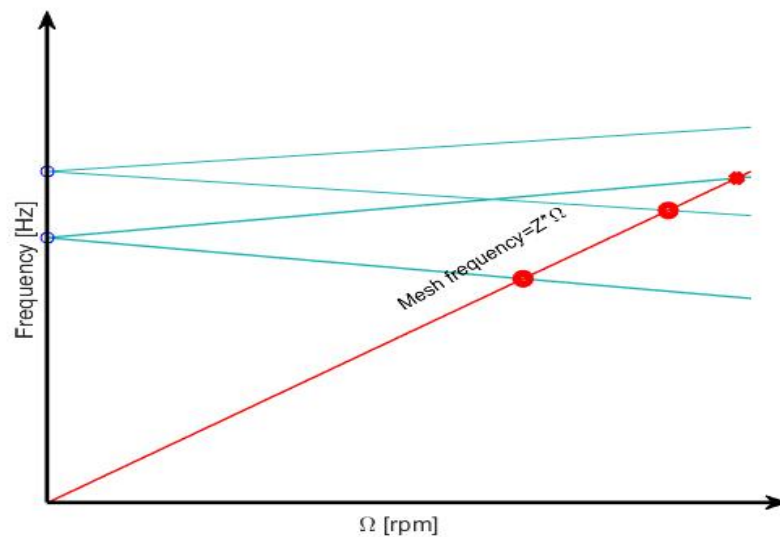


Fig. 5.17. Resonance phenomena

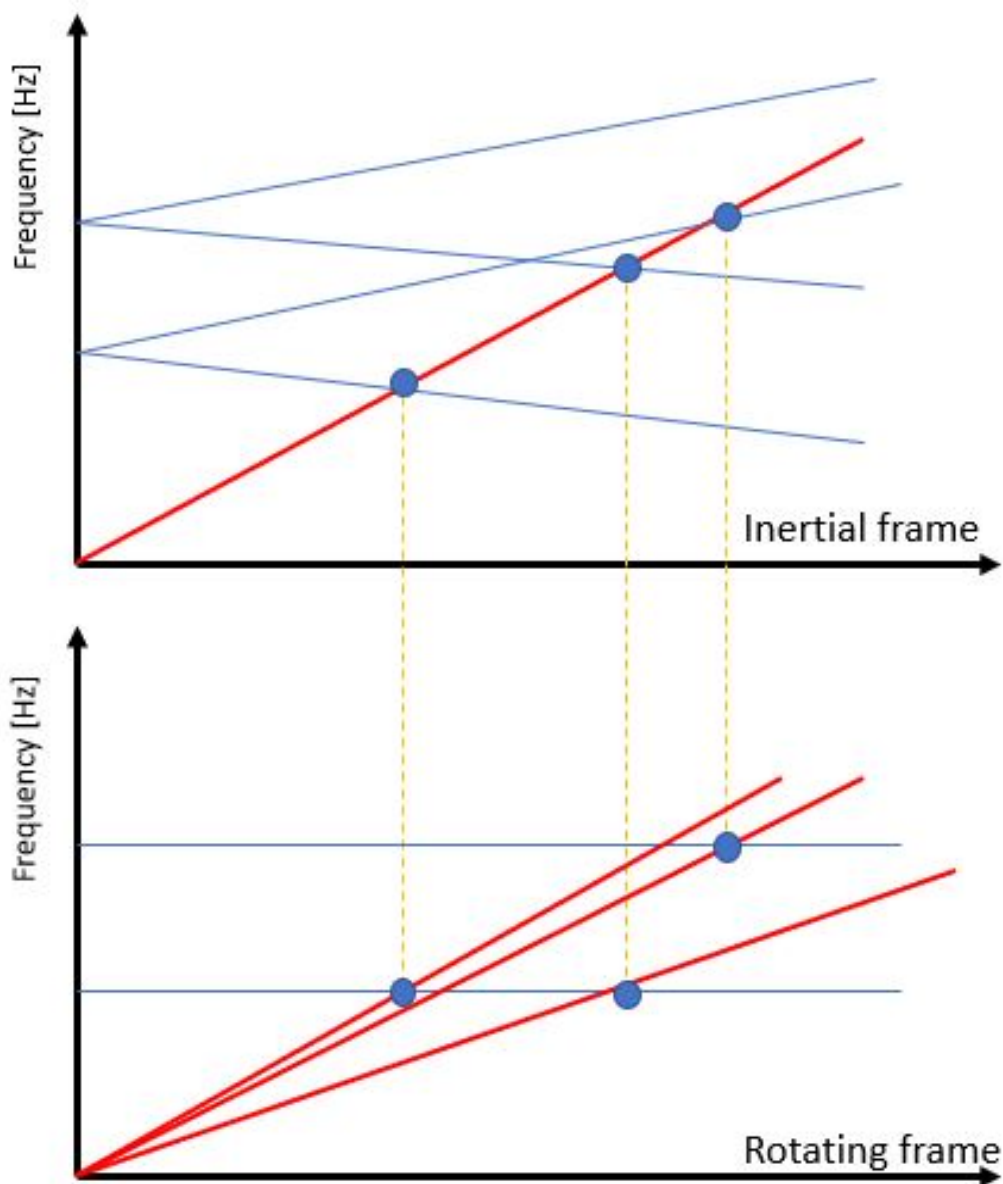


Fig. 5.18. Comparison of Campbell diagram: fixed and rotating frame

All this concerns inertial reference system, if instead, we are in the rotating referencing system, the point of contact is stopped, the one that moves is the load. Therefore, the backward and forward frequencies coincide, this means that the natural frequencies do not open, the one that will open is the mesh frequency.

FRF analysis

We use Modal analysis's results calculated following the process described in Appendix A to calculate frequency response of the helical test case. The unitary excitation force is supposed to be applied perpendicular to the facewidth. Eq.5.10 calculates the frequency response.

$$\begin{bmatrix} x_{10} \\ x_{20} \\ \dots \\ x_{j0} \\ \dots \\ x_{n0} \end{bmatrix} = \sum_{r=1}^n \frac{\begin{bmatrix} \Psi_{1r} & \Psi_{2r} & \dots & \Psi_{jr} & \dots & \Psi_{nr} \end{bmatrix}}{K_r - m_r \Omega^2 + i \Omega c_r} \begin{bmatrix} 0 \\ 0 \\ \dots \\ F_{j0} \\ \dots \\ 0 \end{bmatrix} \begin{bmatrix} \Psi_{1r} \\ \Psi_{2r} \\ \dots \\ \Psi_{jr} \\ \dots \\ \Psi_{nr} \end{bmatrix} \quad (5.10)$$

- X is the frequency response vector
- Ψ represents r-mode eigenvector
- F is the vector of the excitation force
- Ω is the excitation frequency
- k_r :modal stiffness, m_r :mass coefficient and c_r :damping coefficient

Eq. A.7 for a forced system becomes:

$$[M]\ddot{X} + [C]\dot{X} + [K]X = F \quad (5.11)$$

$$X = \sum_{j=1}^N \phi_j \Psi_j \quad (5.12)$$

Thanks Eq.5.12 it is possible to transform Eq. 5.11 in modal coordinates: Eq. A.7 for a forced system becomes:

$$[M]\phi_j \ddot{\Psi}_j + [C]\phi_j \dot{\Psi}_j + [K]\phi_j \Psi_j = F \quad (5.13)$$

Multiplying equation terms for ϕ_j^T :

$$\phi_j^T [M]\phi_j \ddot{\Psi}_j + \phi_j^T [C]\phi_j \dot{\Psi}_j + \phi_j^T [K]\phi_j \Psi_j = \phi_j^T F \quad (5.14)$$

Using orthogonality properties of modal matrix Eq. 5.11 turns into:

$$\ddot{\Psi}_j + 2\zeta_j \omega_j \dot{\Psi}_j + \omega_j^2 \Psi_j = f_j \quad (5.15)$$

It is possible to observe the modes aperture, as explained in Section 5.2.5, even for the frequency response, this phenomena causes duplication of the intersection points between mesh

frequency and natural frequency lines, and this leads obviously to a duplication of the peaks of response in the response diagram referred to as backward and forward resonances shown in Fig.5.19

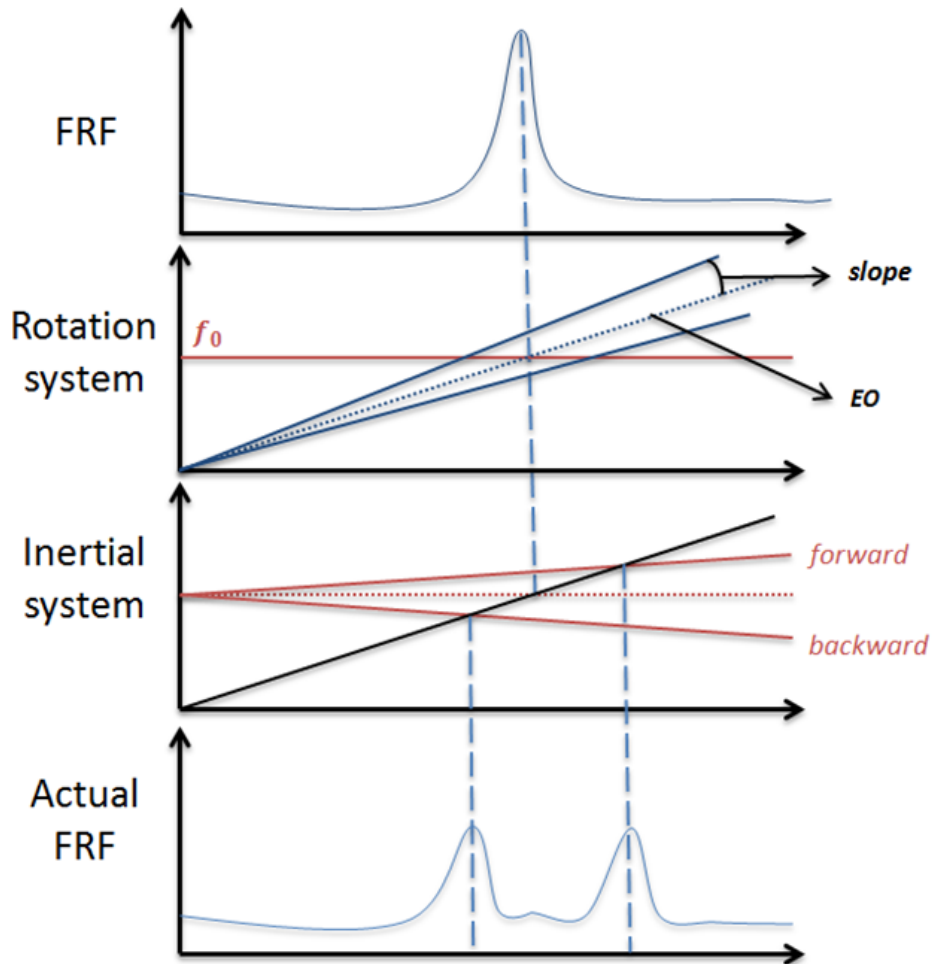


Fig. 5.19. FRF analysis results

RiskFactor calculation

The last step of the setting of Dynamic Topology consist on the calculation of the actual risk factor achieved by HML script. We perform the modal analysis in two set of nodes that consist on one node for each tooth, Fig.5.20, after that we execute the FRF that is the starting point for the calculation of Risk Factor.

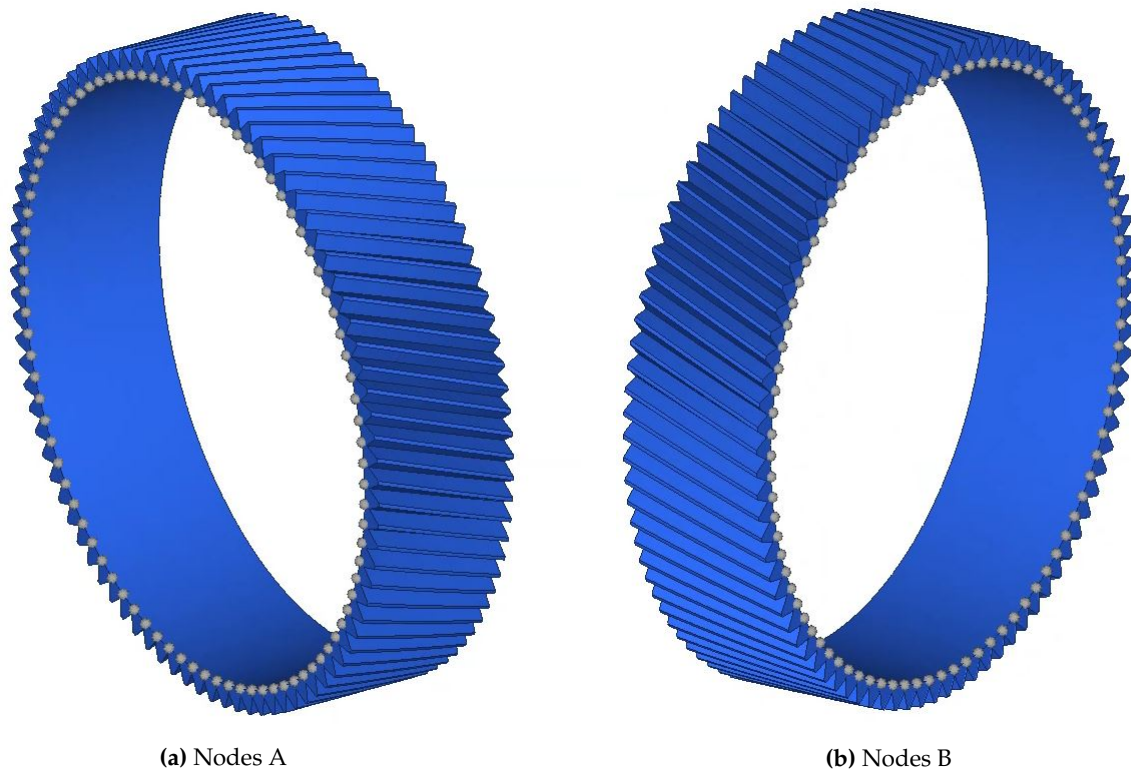


Fig. 5.20. Modal analysis nodes

Thanks to the linear properties of Eq. 5.10 the single responses of each mode extracted by the modal analysis can be summed. Unfortunately, this simple method led to a lack of accuracy in the evaluation of the peaks amplitude because by summing all the responses the average value of the FRF will rise. In addition, if peaks are not so sharp, it is possible that negligible peaks could be considered in the sum with “tails” of bigger ones becoming un-negligible and so invalidating the FRF.

To avoid this mistake, during the Risk Factor calculation we consider the amplitude and the location of these singular identified peaks for each normal mode. Peaks amplitude are normalized so they assume values between zero and one and are stored in a final vector that is the one compared with the Risk Factor function that leads to Risk Factor that can variate between zero and one.

For each engine's operative condition, it can be identified:

- Operative Speed
- Work Range
- Margin Band
- Safety Band

Inside the margin range the Risk Factor assumes the maximum value, instead it is zero outside the safety range and it grows up linearly from zero to one between the safety range and the margin band as shown in Fig.5.21. RF trend leads to a trapezoidal shape of RF envelope for each operative condition.

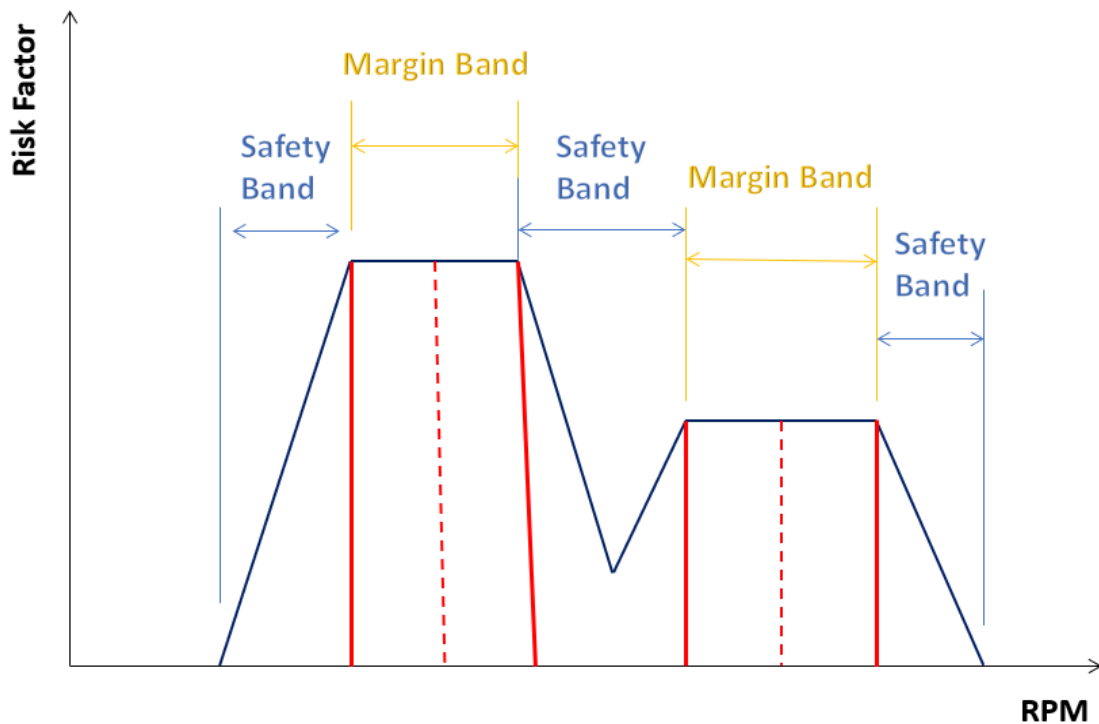


Fig. 5.21. Risk Factor trend

If two operative ranges are near one to the other (in terms of RPM), the margin band or the safety band could overlies, to solve this issue the function is programmed to calculate the envelope of the two-trapezoidal shapes.

To sum up, the dynamical behavior of the gears can be evaluated, in terms of risk of resonance, by a single parameter, named Risk Factor, that is calculated following the method illustrated before and sketched in Fig. 5.22.

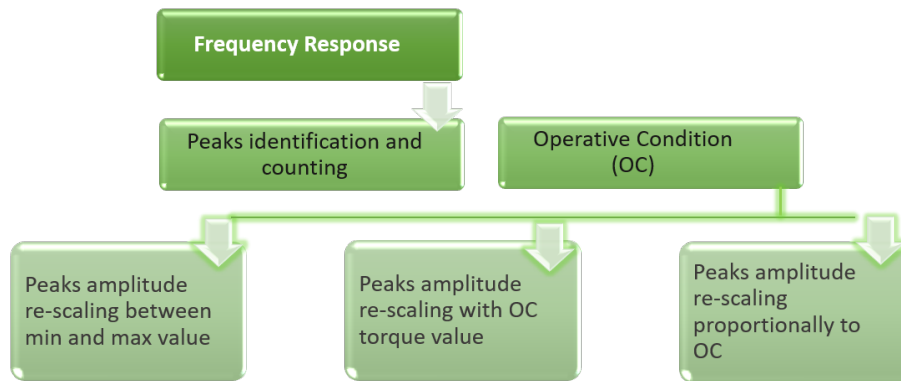


Fig. 5.22. Risk Factor calculation process

As said in Section 5.2.5, the Risk Factor is defined by four parameters, they may be linked together in so many ways according to the how the user wants to set the optimization process. D'Alò established two main methods [5]:

1. Minimize only one of the four components to reduce the total risk.
2. Minimize simultaneously all its component, if one of them tends to zero while another tends to one, the total risk will not change.

For our purposes Risk Factor is passed to the solver as a design constraint and not as an objective function like in the D'Alò project. It's possible to constraint RF by defining a specific range that must be respected by the optimizer; we only allocate the upper limit.

By setting this dynamic constraint we end the implementation of Topology Optimization, as a consequence we can start with optimization analysis.

Optimization results are shown in Section 5.3.

5.3 Post Processing

Once the design variable assigned to the design space's test case will be set, Optistruct will be launched and we will be able to analyze its results that consist on optimized gear.

As mentioned in the introduction this thesis represents the continuation of two previous thesis works, in particular in the second of these dynamic optimization had already been set but once applied to the test case in analysis of this thesis the tool did not work and since numerous adjustments have been made, to check the tool we need to reduce the analysis time so we have moved to a simplified model: RING model.

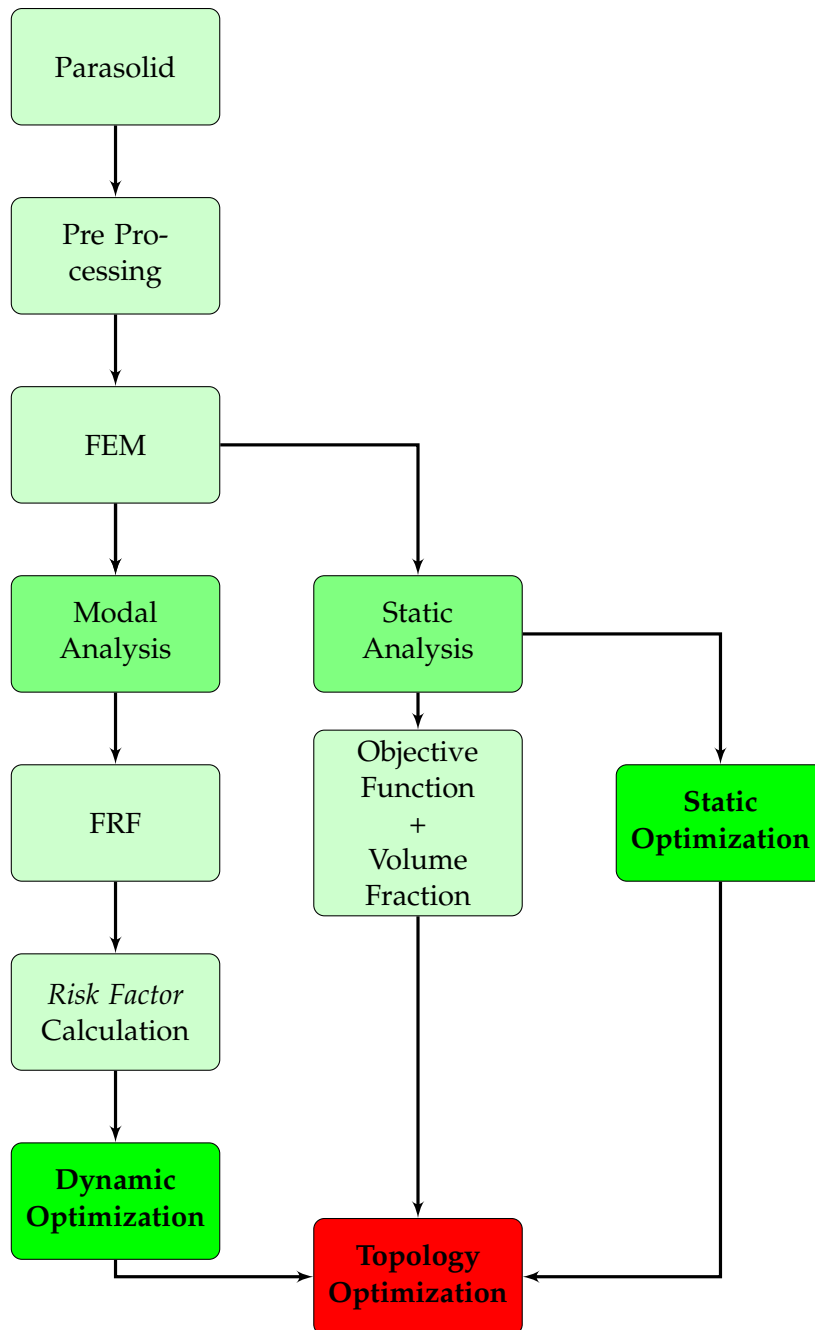


Fig. 5.23. Topology Optimization process

5.3.1 Ring Test Case

In this section we illustrate the results obtained for the simplified model with regard to **Dynamic Optimization**.

We start to calculate the Risk Factor envelop shown in Fig. 5.24.

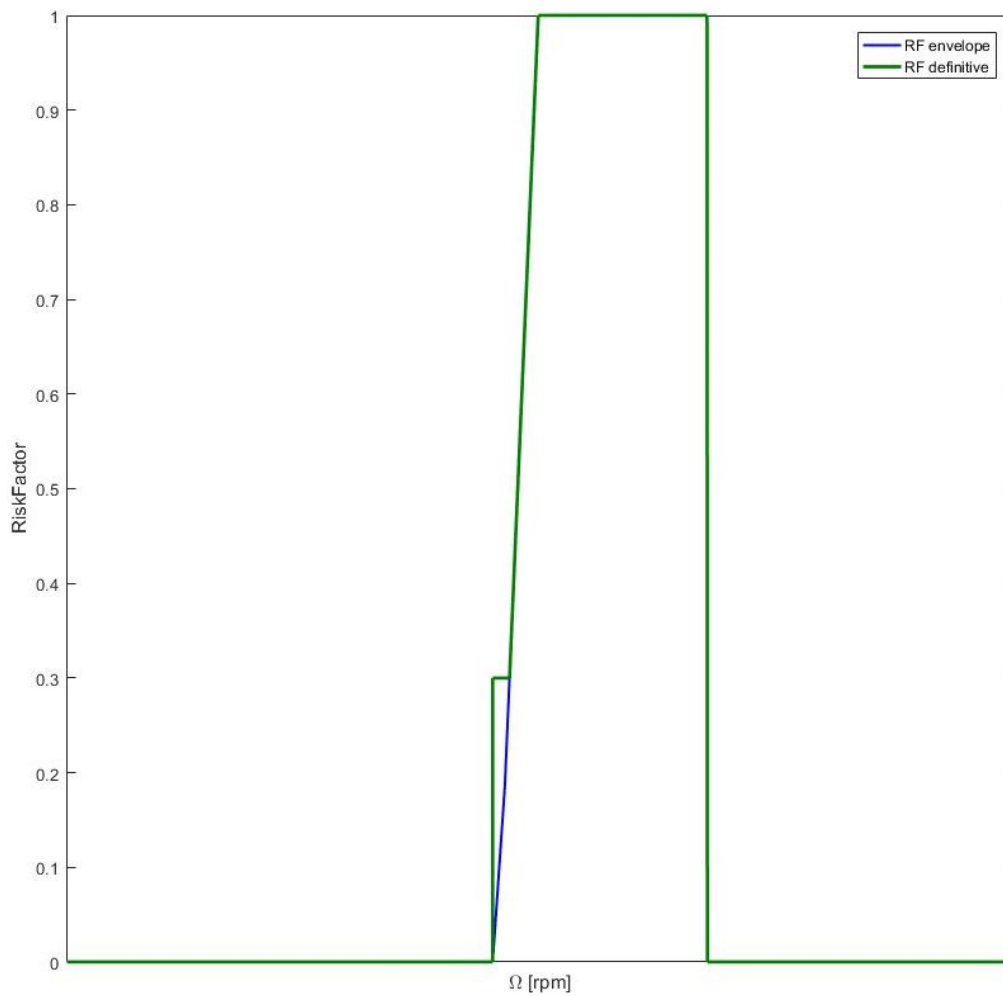


Fig. 5.24. RF envelope

After 89 hours of analysis and 48 Iteration the optimization has converged. Fig. 5.26 displays the last iteration with a density index of 0.3.

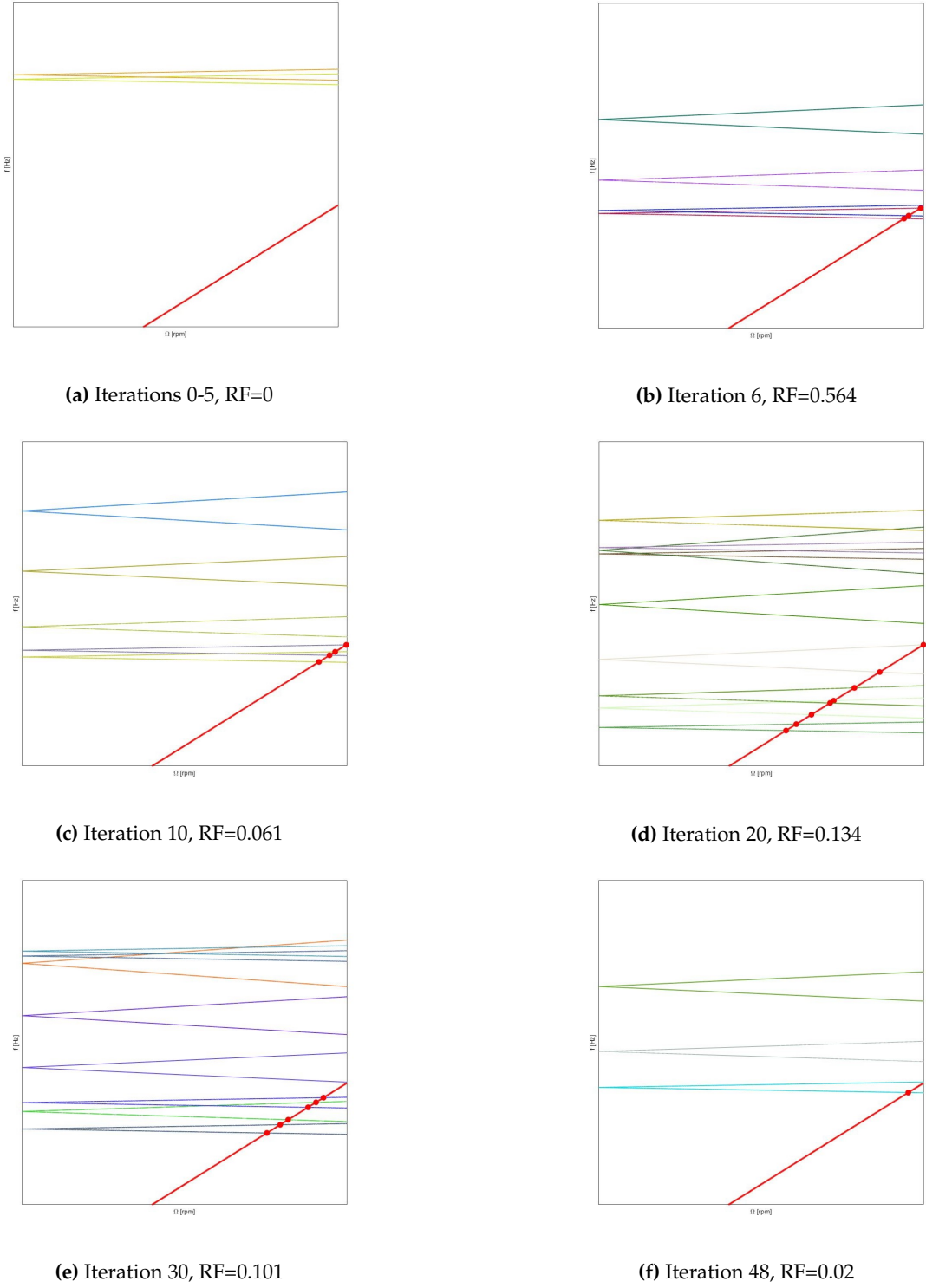


Fig. 5.25. Ring's Campbell diagrams for each iteration

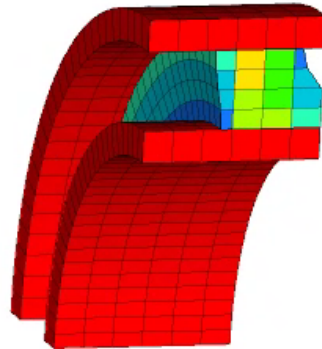


Fig. 5.26. Ring model dynamic optimization

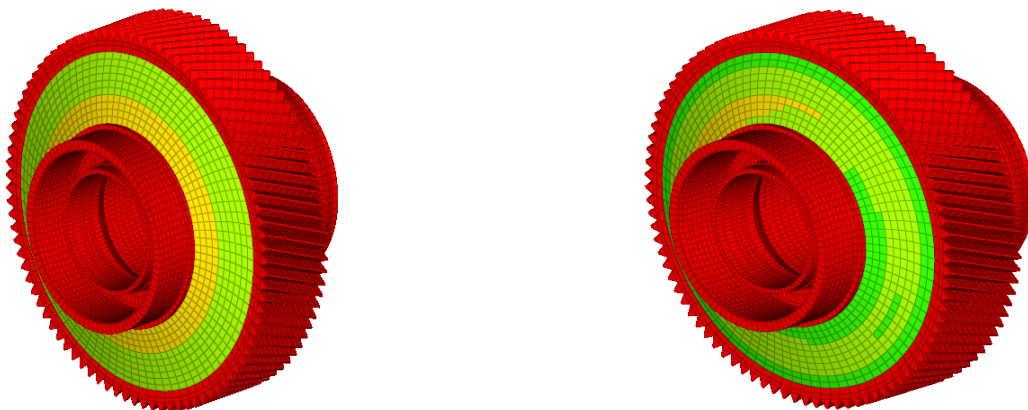
5.3.2 Helical gear test case

It is time to observe test case's results.

Static Optimization

Since the design variable used for this test case can be set up following different design cards as explained in Sections 4.4.6, 5.2.2, in the current section different tests will carry out in order to obtain different results and better understand the function of each manufacturing constraint of interest to set the complete optimization.

We want an axial-symmetrical web so we analyze Pattern Grouping and Extrusion options, Fig.5.27.



(a) Pattern grouping design card

(b) Extrusion design card

Fig. 5.27. Axial-symmetrical design variable

As it is possible to see in Fig.5.27a the Pattern Grouping returns an axial-symmetrical design space, instead we can observe different densities in Fig.5.27b, consequently Extrusion option is discarded.

Let's try now to change the manufacturing constraints.

TABLE 5.2: First set up of Static Optimization, Fig.5.28

| | |
|------------------|-----|
| Pattern Grouping | ON |
| NO HOLE option | OFF |
| OBSTACLE option | ON |

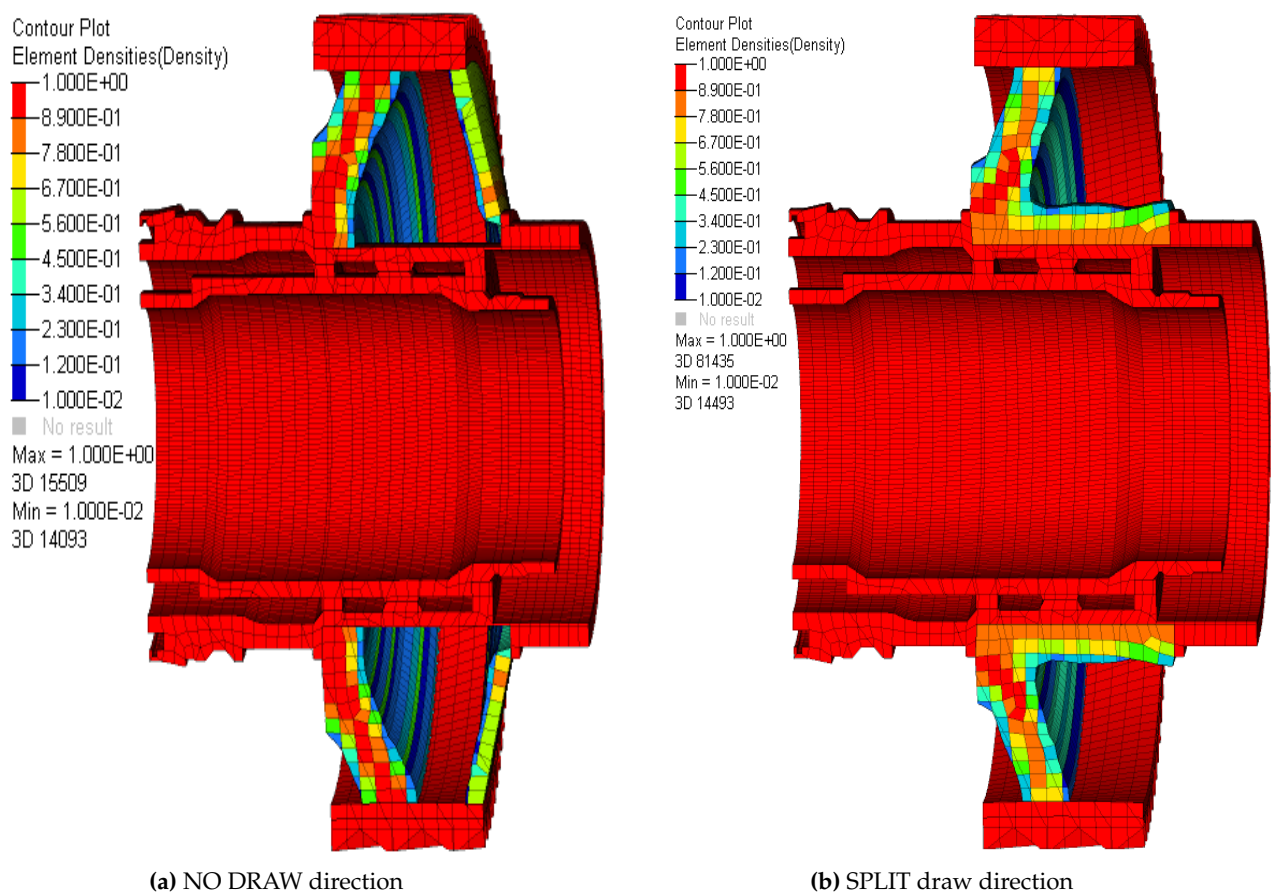


Fig. 5.28. First set up of Static Optimization

TABLE 5.3: NO DRAW design card, Fig. 5.28a

| | |
|-----------------|---------|
| N° ITERATIONS | 16 |
| Running time | 0:19:03 |
| Feasible Design | YES |

TABLE 5.4: SPLIT design card, Fig. 5.28b

| | |
|-----------------|---------|
| N° ITERATIONS | 17 |
| Running time | 0:28:24 |
| Feasible Design | YES |

TABLE 5.5: Second set up of Static Optimization

| | |
|------------------|----|
| Pattern Grouping | ON |
| DRAW direction | ON |
| NO HOLE option | ON |
| OBSTACLE option | ON |

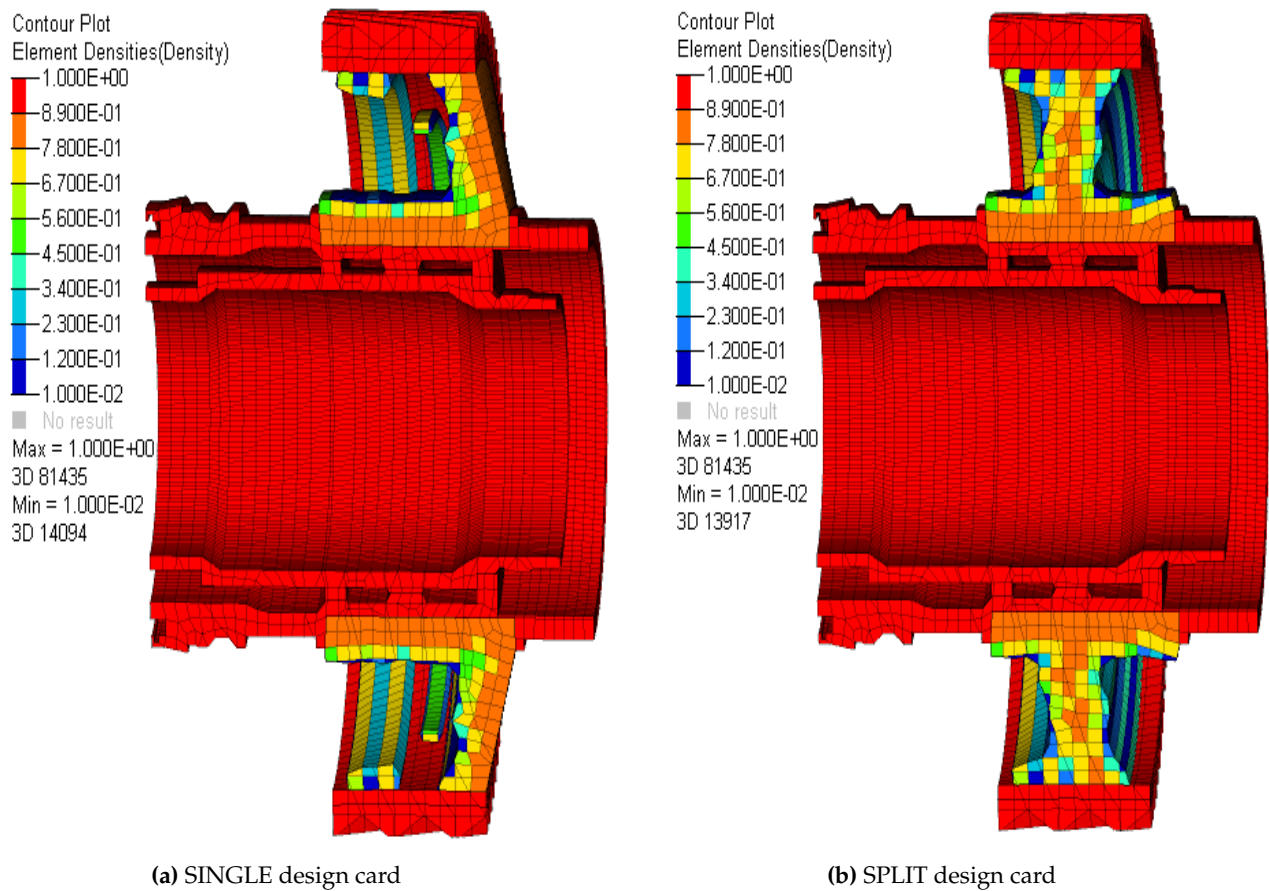


Fig. 5.29. Second set up of Static Optimization

TABLE 5.6: SINGLE design card, Fig. 5.29a

| | |
|------------------|---------|
| N° ITERATIONS: | 24 |
| Running time: | 0:31:16 |
| Feasible Design: | NO |

TABLE 5.7: SPLIT design card, Fig. 5.29b

| | |
|------------------|---------|
| N° ITERATIONS: | 25 |
| Running time: | 0:27:46 |
| Feasible Design: | YES |

Dynamic Optimization

The topology optimization of the bevel gear discussed in this section considers only the dynamical design constraints implemented like in Fig.5.30.

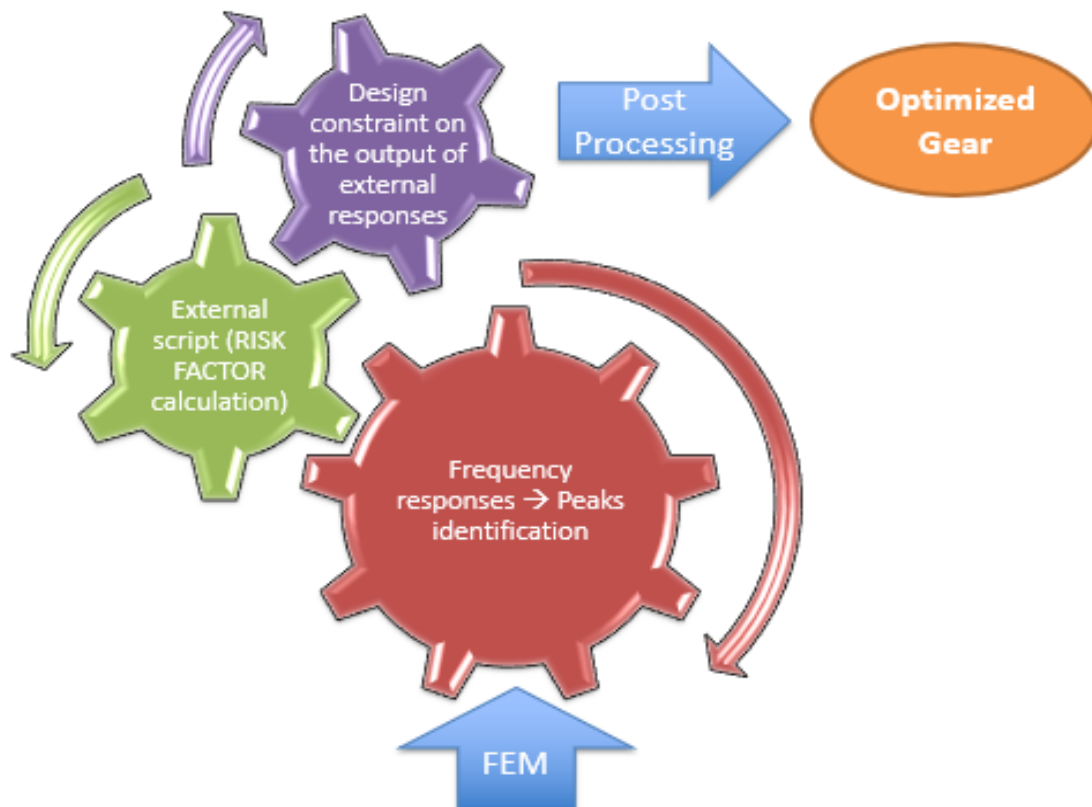


Fig. 5.30. Dynamic Topology Optimization process

The dynamic forces that excite the test case are those deriving from the engagement. These forces must be expressed in a rotating reference system where the meshing forces are rotating loads which act on all the teeth of the gear with a time profile phase shifted of a time Δt between a gear and the respective one and they are related to the rotational speed Ω and the number of teeth Z .

$$\Delta t = \frac{2\pi}{Z\Omega} \quad (5.16)$$

The profile of meshing force is different from zero in a small portion of the graph that corresponds to the condition of loaded tooth.

Helical gear's results are represented in Fig.5.31.

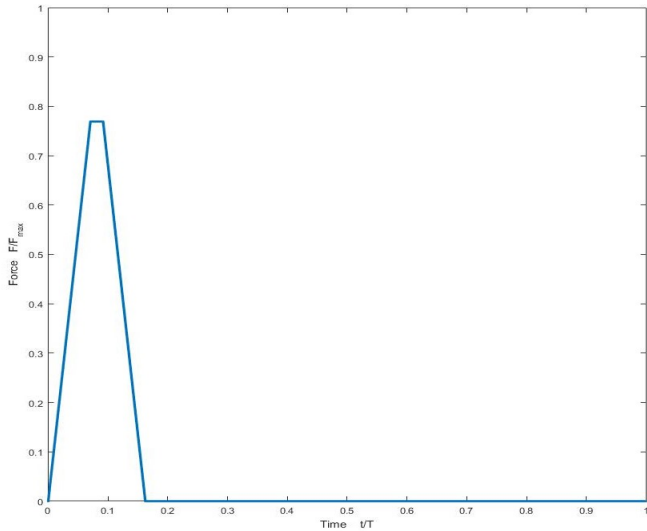


Fig. 5.31. Engagement force profile over a period T

The temporal profile of the forcing can be developed by Fourier series to calculate the spectrum as illustrated in Fig.5.32.

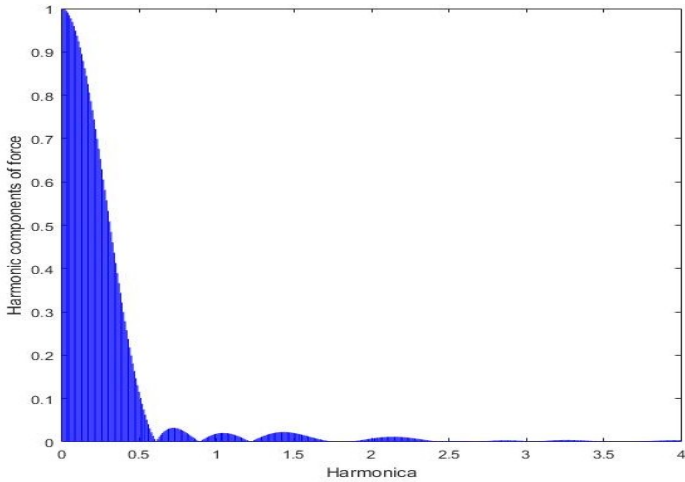


Fig. 5.32. Frequency spectrum of the excitation force

Once the spectrum has been calculated, the harmonic component to be selected is the one corresponding to the engine order number that excites the resonance. The choice between all the possible values will depend on which intersection between forward and backward lines and mesh frequency curves on the Campbell diagram.

To well analyze gear dynamic, we must consider a great number of responses but this means that the calculation time increase, in fact for this test case the solver needs approximately 10 hours for each iteration.

TABLE 5.8: Dynamic Optimization set up

| | |
|------------------|--------|
| Pattern Grouping | ON |
| DRAW direction | SINGLE |
| NO HOLE option | ON |
| OBSTACLE option | OFF |

We start to calculate the Risk Factor envelop shown in Fig. 5.33.

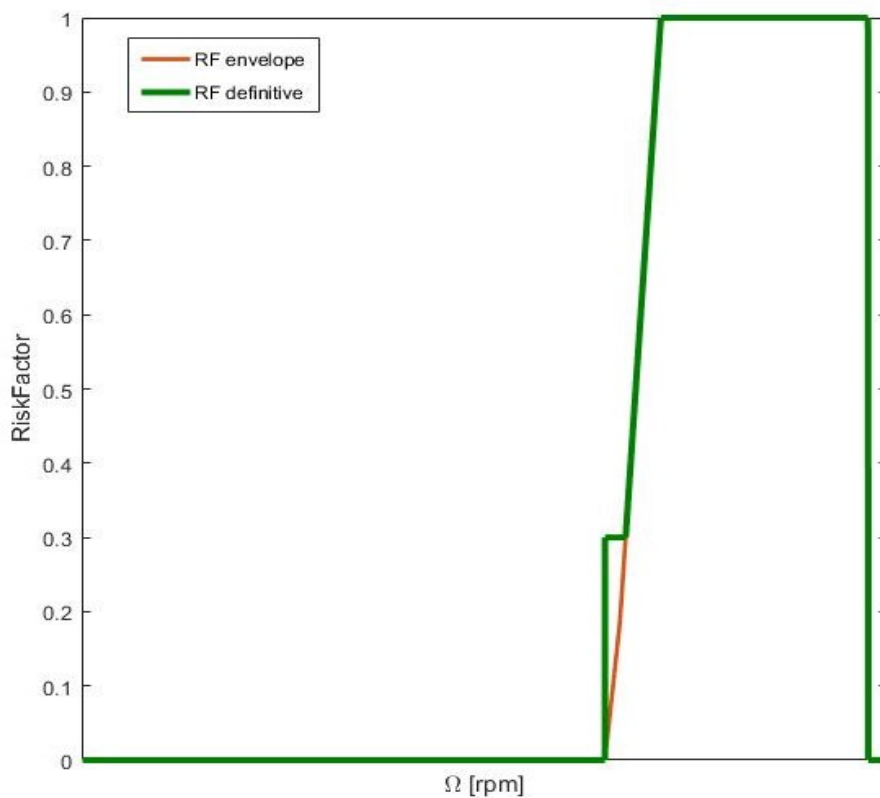


Fig. 5.33. RF envelope of Test Case

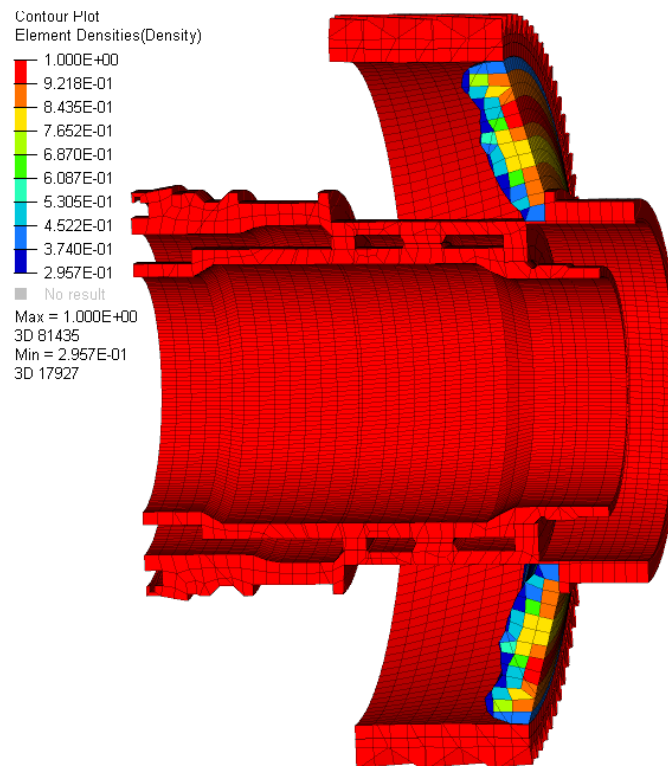


Fig. 5.34. Dynamic Topology Optimization of helical gear

Combined Topology Optimization

In this final section the helical gear test case will be optimized considering both the Static and the Dynamic design constraints. Before showing the Optimization results Campbell diagram would be displayed.

By observing only static, Fig. 5.29a, and only dynamic optimization, Fig. 5.34, we can see that if we do not add obstacle card to dynamic optimization the new design sometimes does not connect with gear's teeth, this is because we perform modal analysis, instead static optimization does not care about this design option because the teeth and the web need to be connected to face the contact force.

So, if we implement static and dynamic separately and we want a realistic web design we must use this option only in dynamic optimization, but if we accomplish complete topology optimization obstacle card is not necessary, consequently the first analysis is run without draw options.

To perform Complete Optimization we need long time running analysis so we will not able to check all the design option, this is the reason why we decide to not constrain the design direction to see which is the shape that the solver gives us without any constraints and we perform

this choice because as it is possible to see in Tables. 5.3.2, 5.4, 5.6, 5.7 NO DRAW design direction analysis needs less time and iteration then others.

Our goal is to understand if the resulting shape of the Complete Optimization would be completely different from static one, Fig. 5.28a.

TABLE 5.9: Combined Optimization set up

| OBJECTIVE FUNCTION | MIN COMPLIANCE |
|--------------------|----------------|
| VOLUME FRACTION | 0.3 |
| STATIC CONSTRAINTS | ON |
| RISK FACTOR | 0.4 |
| Pattern Grouping | ON |
| DRAW direction | OFF |

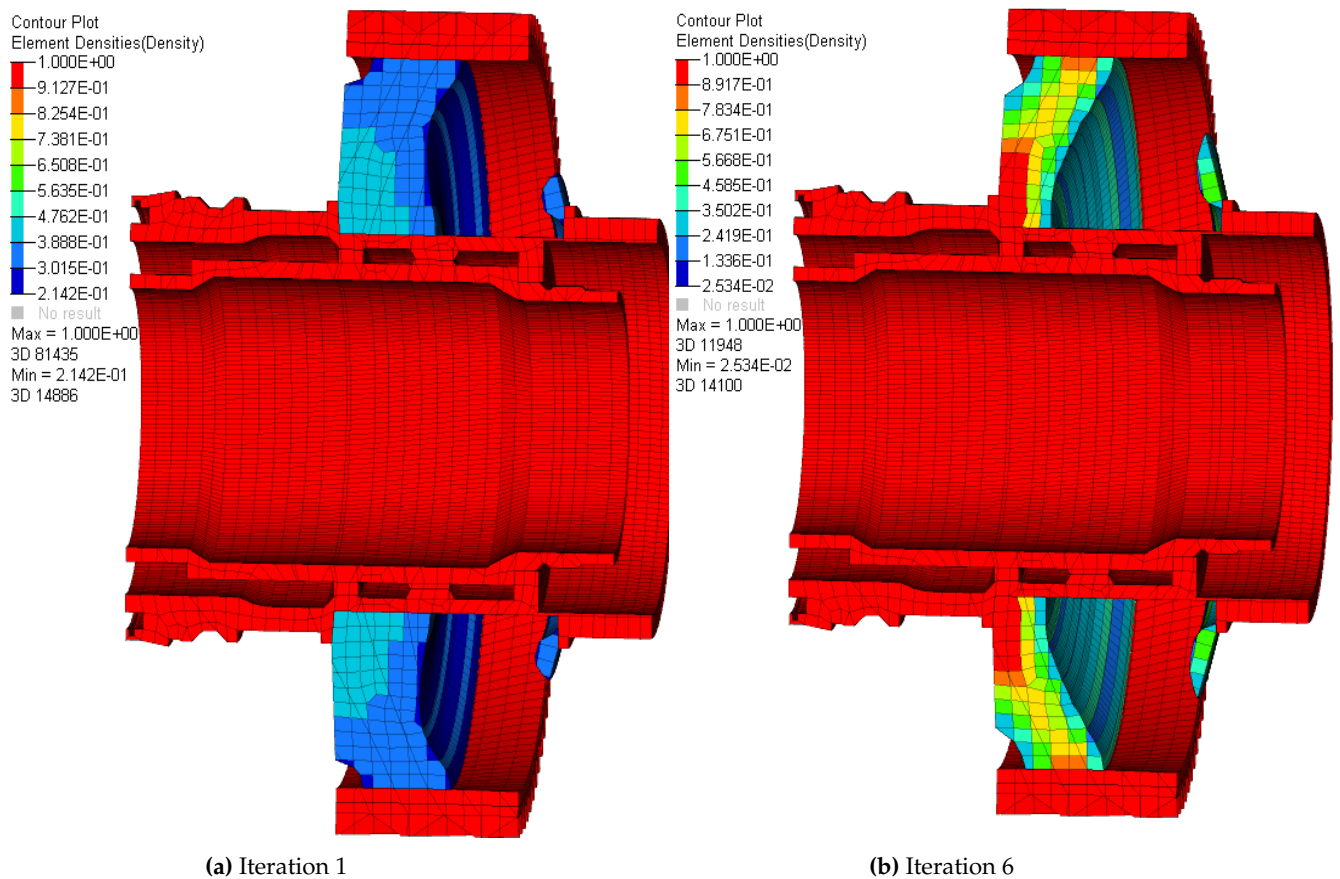


Fig. 5.35. Intermediate iterations of Helical gear's Combined Optimization

Table 5.10 contains the result of the combined topology optimization and in Fig. 5.36 displays the last iteration with a density index of 0.3.

TABLE 5.10: Combined optimization results

| | |
|-----------------|-----------|
| N° ITERATIONS | 42 |
| Running time | 366:17:00 |
| Feasible Design | NO |

The solver converged to the unfeasible design shown above. The reasons of this failure are identified in the output file provided by Optistruct.

The dynamic constraint seems to be too restrictive.

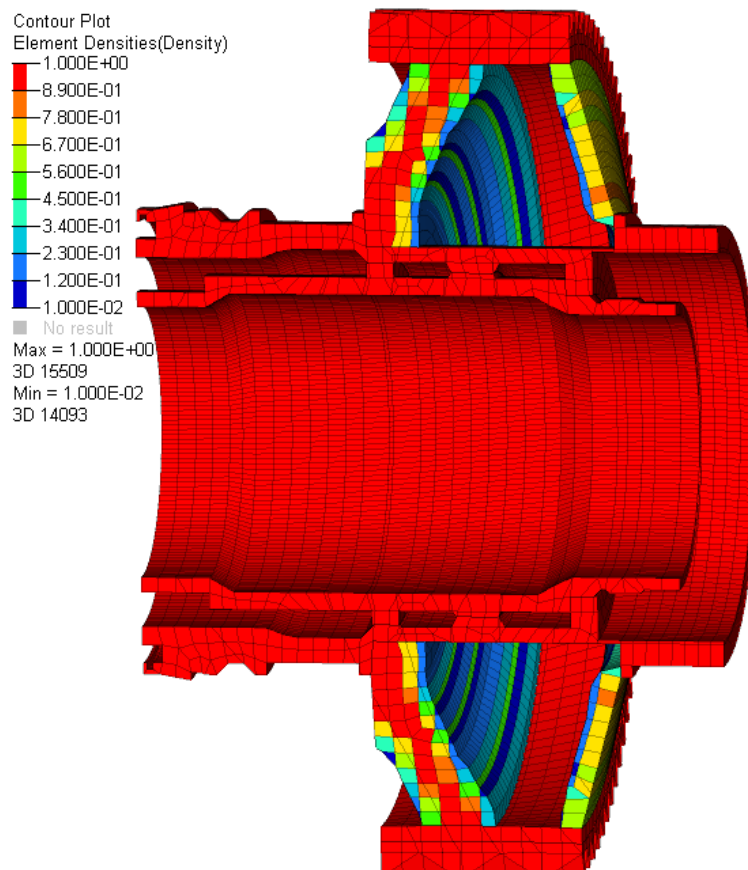
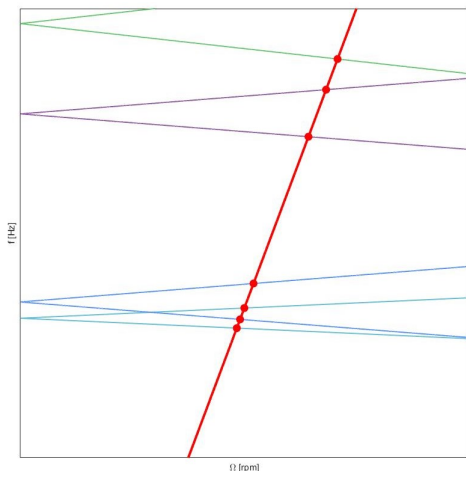


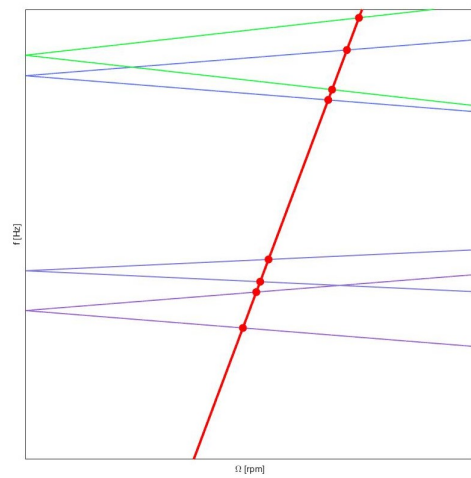
Fig. 5.36. Combined Topology Optimization of helical gear

To confirm that the tool works well we print the Campbell diagram, described in Sec. 5.2.5. As it is possible to see in Fig. 5.37 the crossing points, that show the resonance frequencies, become greater with the increasing of Risk Factor value.

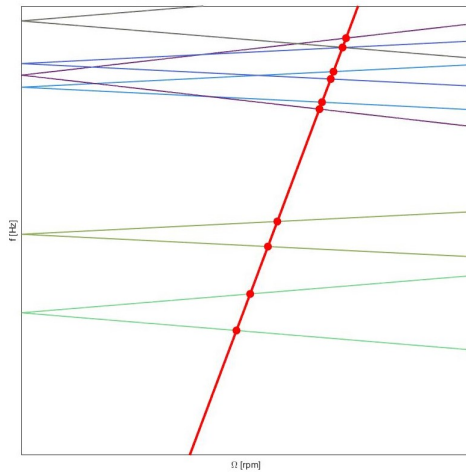
The tool is validated, it well computes gears' dynamic.



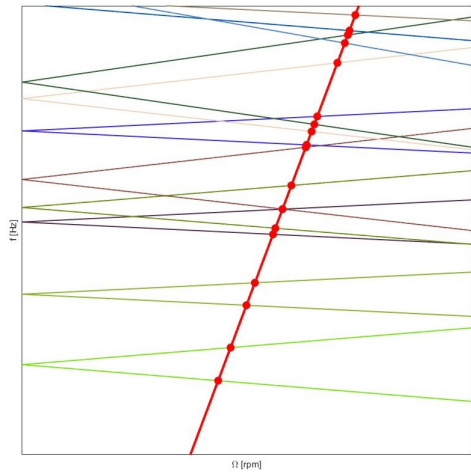
(a) Iteration 0, RF=0.334



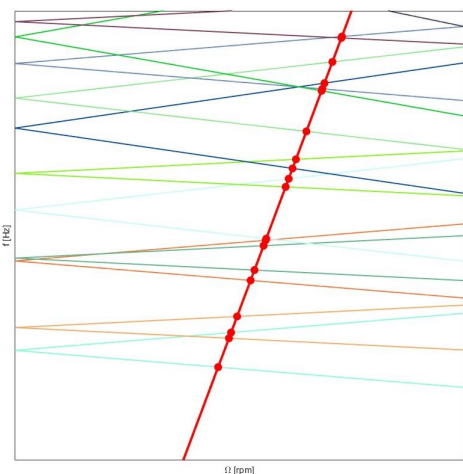
(b) Iteration 1, RF=0.465



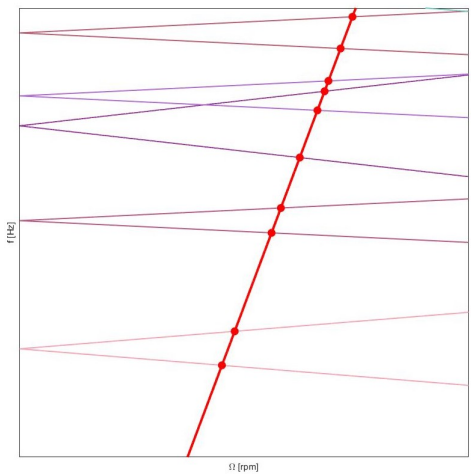
(c) Iteration 9, RF=0.593



(d) Iteration 23, RF=0.669



(e) Iteration 33, RF=0.4687



(f) Iteration 42, RF=0.532

Fig. 5.37. Helical gear's Campbell diagrams for each iteration

Chapter 6

Conclusions

This thesis shows that it is possible to implement in Optistruct working space custom optimizations, rotating components' static and dynamic topology optimizations were implemented.

The method output is a new design that respects all static and dynamic constraints and it is lighter than the original one and thanks to topology objective we gain the 64% in terms of stiffness. As a consequence, it is proved that this approach is useful during gear's preliminary design, but it is fundamental to remember that the design obtained is not the definitive one. The resulting component must be redefined in a CAD environment for a detailed design, reintroducing all those parts avoided during defeaturing phase. One of the goal reached in this work is the generalization of the tool for any kind of gear, spur, bevel, and helical gears and with any number of teeth, so now it is possible to enter few parameters, such as number of teeth, angles values and damping, to completely set the Dynamic Topology Optimization.

As said before we set a realistic static topology optimization but it can be improved by considering contact print distributed along all the tooth side.

As future developments for this test case it would be interesting to see how gear's shape changes by setting different manufacturing constraints, and if it is possible to obtain a feasible design by just modifying design directions or it is necessary to loosen static and dynamic constraints.

Once the topology optimization converged it is necessary to consider gear fatigue, the setting of fatigue issue represents one of the next progresses of this thesis.

If future software's versions will allow the use of properties related to cyclic symmetry it will be possible to use an alternative way to calculate RiskFactor to investigate gears' dynamic behavior using DRESP2 responses instead of external DRESP3.

Appendix A

Modal Analysis

The motion of a dynamic structure or system may be represented by a set of simultaneous differential equations using some discretization schemes, such as the finite element method. Dynamic responses, strains, stresses that are the dynamic characteristics of the system can be obtained from differential equations using the direct integration methods such as finite difference method or Newmark method in the time domain. On the other hand, these coupled equations of motion may be solved by transforming them into a set of independent (uncoupled) equations by means of a modal matrix, that procedure consists in modal analysis calculation. Modal analysis is composed by the calculation of system's modal parameters, including natural frequency, natural mode, damping factor, modal scaling. The determination of these modal parameters could be theoretical (analytical or numerical) or experimental.

Theoretical modal analysis was developed during the 19th century. At that stage, the analytical approaches were used to solve differential equations to determine the modal parameters. During the last century, the theoretical modal analysis for the complex and large systems made great progress with the fast development of the discretization technique (finite element method) and computer techniques. Since then, numerical rather than analytical methods have been commonly used in the modal analysis, called numerical modal analysis.

Experimental modal analysis started in the early 1900s thanks to electrical engineering development and it is based on system identification. The development of fast Fourier transform (FFT) by Cooley and Tukey in 1965 was the guiding light of the experimental modal analysis. Sometimes it is not possible to describe elastic systems with only one mass, but they need to be represented by systems of two or more masses thought as point masses or particles having no rotational inertia. If a group of particles is bound together by essentially rigid connections, it behaves as a rigid body having both mass (significant for translational motion) and moment of inertia (significant for rotational motion). There is no limit to the number of masses that may be used to represent a system. For example, each mass in a model representing a beam may be an infinitely thin slice representing a cross section of the beam; a differential equation is required to treat this continuous distribution of mass.

The number of independent parameters required to define the distance of all the masses from their reference positions is called the number of degrees-of-freedom N . For example, if

there are N masses in a system constrained to move only in translation in the X and Y directions, the system has $2N$ degrees-of-freedom. Instead, a continuous system such as a torsional beam has a great number of degrees-of-freedom. Each coordinate of motion of each mass that means each degree-of-freedom is associated to a differential equation written as:

$$m_j \ddot{x}_j = F_{xj} \quad I_k \ddot{\alpha}_k = M_{\alpha k} \quad (\text{A.1})$$

Where F_{xj} is the component in the X direction of all external, spring, and damper forces acting on the mass having the j th degree-of-freedom, and $M_{\alpha k}$ is the component about the α axis of all torques acting on the body having the k -th degree-of-freedom. The moment of inertia of the mass about the α axis is designated by I_k .

A.1 Free vibration Systems

System oscillates under the action of forces inherent in the system itself and in absence of externally applied forces. The system will vibrate at one or more of its natural frequencies, which are properties of the dynamical system established by its mass and stiffness distribution. The response of a system is called free vibration when it is disturbed and then left free to vibrate about some mean position.

A.1.1 Single Degree of Freedom System

A single-degree-of-freedom (SDOF) system (see Fig. A.1) where the mass m can only move along the vertical x -axis is described by the following equation:

$$m\ddot{x}(t) + c\dot{x}(t) + kx(t) = 0 \quad (\text{A.2})$$

With m the mass, c the damping coefficient, and k the stiffness. This equation states that the sum of all forces acting on the mass m should be equal to zero with $f(t)$ an externally applied force, $-m\ddot{x}(t)$ the inertial force, $-c\dot{x}(t)$ the (viscous) damping force, and $-kx(t)$ the restoring force. The variable $x(t)$ stands for the position of the mass m with respect to its equilibrium point, i.e. the position of the mass when $f(t) \equiv 0$. When A.2 is transformed to the Laplace domain (assuming zero initial conditions) becomes:

$$Z(s)X(s) = F(s) \quad (\text{A.3})$$

Where $Z(s)$ is the dynamic stiffness $\rightarrow Z(s) = ms^2 + cs + k$. The transfer function $H(s)$ between displacement and force, $X(s) = H(s)F(s)$, corresponds to the inverse of the dynamic stiffness.

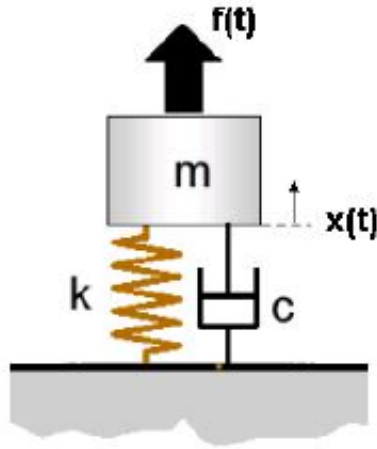


Fig. A.1. SDOF system [6]

$$H(s) = \frac{1}{ms^2 + cs + k} \quad (\text{A.4})$$

The poles of the systems are the roots of the denominator of the transfer function $d(s) = ms^2 + cs + k$. The damping coefficient c of mechanical structures is very small deriving from complex conjugate pole pair.

$$\lambda = -\sigma \pm i\omega_d \quad (\text{A.5})$$

With:

- $f_d = \frac{\omega_d}{2\pi}$ the damped natural frequency,
- $f_n = \frac{\omega_n}{2\pi}$ the (undamped) natural frequency where $\omega_n = \sqrt{\frac{k}{m}} = |\lambda|$
- $\zeta = \frac{c}{2m\omega_n} = \frac{\sigma}{|\lambda|}$ the damping ratio ($f_d = f_n \sqrt{1 - \zeta^2}$)

When a mass Δm is added to the original mass m of the structure, its natural frequency decreases to $\omega_n = \sqrt{\frac{k}{m + \Delta m}}$. If $c = 0$, the system is not damped and the poles becomes purely imaginary, $\lambda = \pm i\omega_n$.

The Frequency Response Function (FRF), denoted by $H(\omega)$, is obtain by replacing the Laplace variable s in Eq. A.4 by $i\omega$ resulting in:

$$H(s) = \frac{1}{-m\omega^2 + ic\omega + k} = \frac{1}{(k - im\omega^2) + ic\omega} \quad (\text{A.6})$$

Clearly, if $c = 0$, then $H(\omega)$ goes to infinity for $\omega \rightarrow \omega_n = \sqrt{\frac{k}{m}}$ how it is possible to see in Fig. A.1.

Although very few practical structures could realistically be modeled by a single-degree-of-freedom (SDOF) system, the properties of such a system are important because those of a more complex multiple-degree-of-freedom (MDOF) system can always be represented as the linear superposition of a number of SDOF characteristics (when the system is linear time-invariant).

A.1.2 Multiple Degree of Freedom System

Multiple-degree-of-freedom (MDOF) systems are described by the following equation:

$$M\ddot{x}(t) + C\dot{x}(t) + Kx(t) = f(t) \quad (\text{A.7})$$

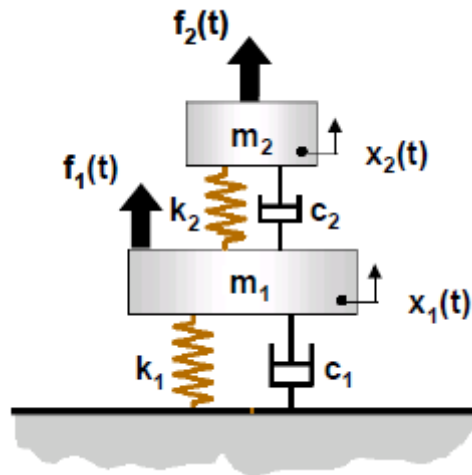


Fig. A.2. 2-DOF system. [6]

Following equations represent the different matrices that are defined for a 2-DOF system, shown in Fig A.2.

$$M = \begin{bmatrix} m_1 & 0 \\ 0 & m_2 \end{bmatrix}$$

$$K = \begin{bmatrix} k_1 + k_2 & -k_2 \\ -k_2 & k_2 \end{bmatrix}$$

$$C = \begin{bmatrix} c_1 + c_2 & -c_2 \\ -c_2 & c_2 \end{bmatrix}$$

$$x(t) = \begin{bmatrix} x_1(t) \\ x_2(t) \end{bmatrix} \quad f(t) = \begin{bmatrix} f_1(t) \\ f_2(t) \end{bmatrix} = \begin{bmatrix} 0 \\ 0 \end{bmatrix}$$

Suppose that the example two-DOF system is undamped:

- $c = c = 0$, whence $C = 0$, the null 2×2 matrix.
- $f_1 = f_2 = 0$, whence $f(t) = 0$, the null 2×1 vector \rightarrow *unforced system*.

The Eq. A.7 reduces to

$$M\ddot{x}(t) + Kx(t) = 0 \quad (\text{A.8})$$

Equation A.8 is a set of n simultaneous homogeneous differential equations. Generally, the solution of Eq. A.8 has the form:

$$x(t) = \phi \sin(\omega t + \alpha) \quad \text{or} \quad x(t) = \phi e^{i\omega t} \quad (\text{A.9})$$

Where ϕ is the vector of amplitudes, ω is the frequency of harmonic response, and α is the phase angle. Differentiation of Eq. A.9 twice with respect to time produces

$$\ddot{x}(t) = -\omega^2 \phi \sin(\omega t + \alpha) \quad (\text{A.10})$$

Substituting A.9 and A.10 into Eq. A.8 and rearranging it results in

$$[K - \omega^2 M] \psi = 0 \quad (\text{A.11})$$

Now, the n simultaneous homogeneous differential equations are reduced to a set of n homogeneous algebraic equations. Equation A.11 has the form of an algebraic eigenvalue problem usually it is named an eigenproblem. To find nontrivial solutions the determinant of the coefficient matrix must be equal to zero:

$$|K - \omega^2 M| = 0 \quad (\text{A.12})$$

The above equation leads to a polynomial of order n in ω^2 that possesses, in general, n distinct roots. These roots, denoted by $\omega_1^2, \omega_2^2, \dots, \omega_n^2$ or $\lambda_1, \lambda_2, \dots, \lambda_n$ are called *eigenvalues*. Their square roots are called *natural frequencies*. Associated with each eigenvalue ω_i^2 , there is an n -dimensional vector ϕ_i whose elements are real numbers. The vector can be obtained by using A.11 as follows:

$$[K - \omega_i^2 M] \psi_i = 0 \quad (\text{A.13})$$

The vector ψ_i ($i = 1, 2, \dots, n$) is known as an *eigenvector* or modal vector and has the form

$$\phi_i = [\phi_{1i}, \phi_{2i}, \dots, \phi_{ni}]^T \quad (\text{A.14})$$

The eigenvector is also referred to as *mode shape* or *natural mode* because it represents the shape of vibration. All the components of the mode shape are real numbers with only a sign and amplitude difference between any two of them. The phase relationships are either in phase or out-of-phase in 180 degrees. Thus, these mode shapes are also called *real modes*. When the system is undamped natural modes have well defined modal points or lines because all points on the structure pass through their equilibrium positions at the same time.

A.2 Forced System

Forced vibration refers to the motion of the system which occurs in response to a continuing excitation whose magnitude varies sinusoidally with time. The excitation may be, alternatively, force applied to the system (generally, the force is applied to the mass of a single degree-of-freedom system) or motion of the foundation that supports the system. The resulting response of the system can be expressed in different ways, depending upon the nature of the excitation and the use to be made of the result:

1. If the excitation is a force applied to the mass of the system shown in Fig. A.3, the result may be expressed in terms of:
 - The amplitude of the resulting motion of the mass \rightarrow '*motion response*'
 - The fraction of the applied force amplitude that is transmitted through the system to the support. \rightarrow '*force transmissibility*'
2. If the excitation is a motion of the structure, the resulting response usually is expressed in terms of the amplitude of the motion of the mass relative to the amplitude of the motion of the structure. \rightarrow '*motion transmissibility*'

Mostly, the response and transmissibility relations are functions of the forcing frequency and these two parameters change according to different types and degrees of damping.

The following general Eq. A.15 summarizes all kinds of responses of linear systems to a sinusoidal excitation including excitation by external forces or foundation motion, viscous or structural damping, rotational and translational degrees-of-freedom, and from one to an infinite number of degrees-of-freedom:

$$x_k = \sum_{n=1}^N \sqrt{D_{kn}} \omega_n^2 \frac{F_n}{m_n} R_n \sin(\omega t - \theta_n) \quad (\text{A.15})$$

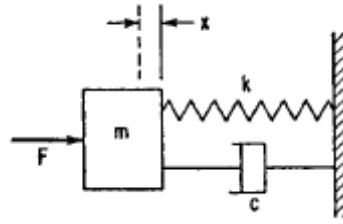


Fig. A.3. Single degree-of-freedom system with viscous damping, excited in forced vibration by force acting on mass.

Where:

x_k = displacement of structure in k^{th} degree-of-freedom

N = number of degrees-of-freedom, including those of the foundation

D_{kn} = amplitude of k th degree-of-freedom in n th normal mode

F_n = generalized force for n th mode

m_n = generalized mass for n th mode

R_n = response factor, a function of the frequency ratio ω/ω_n

θ_n = phase angle

A.2.1 Single Degree of Freedom System

The differential equation of motion for the single degree-of-freedom system with viscous damping shown in Fig.A.3, when the excitation is a force $F = F_0 \sin(\omega t)$ applied to the mass, is:

$$m\ddot{x} + c\dot{x} + kx = F_0 \sin(\omega t) \quad (\text{A.16})$$

Eq. A.16 corresponds to Eq. A.2 for forced vibration of an undamped system. The resulting motion occurs at the forcing frequency ω ; when the damping coefficient c is greater than zero, the phase between the force and resulting motion is different than zero. Thus, the response may be written as

$$x = R \sin(\omega t - \theta) = A_1 \sin(\omega t) + B_1 \cos(\omega t) \quad (\text{A.17})$$

Substituting this relation in A.16, the following result is obtained:

$$\frac{x}{\frac{F_0}{k}} = \frac{\sin(\omega t - \theta)}{\sqrt{\left(1 - \frac{\omega^2}{\omega_n^2}\right)^2 + \left(\frac{2\zeta\omega}{\omega_n}\right)^2}} = R_d \sin(\omega t - \theta) \quad (\text{A.18})$$

where

$$\theta = \tan^{-1} \left(\frac{2\zeta\omega/\omega_n}{\left(1 - \frac{\omega^2}{\omega_n^2}\right)} \right) \quad (\text{A.19})$$

and R_d is a dimensionless response factor giving the ratio of the amplitude of the vibratory displacement to the spring displacement that would occur if the force F were applied statically. At very low frequencies R_d is approximately equal to 1; it rises to a peak near ω_n and approaches zero as ω becomes very large. The displacement response is defined at these frequency conditions as follows:

$$\begin{aligned} x &\simeq \left(\frac{F_0}{k}\right) \sin(\omega t) & [\omega \ll \omega_n] \\ x &= \frac{F_0}{k\zeta} \sin\left(\omega_n t + \frac{\pi}{2}\right) = -\frac{F_0 \cos(\omega_n t)}{c\omega_n} & [\omega = \omega_n] \\ x &\simeq \frac{\omega_n^2 F_0}{\omega^2 k} \sin(\omega t + \pi) = \frac{F_0}{m\omega^2} \sin(\omega t) & [\omega \gg \omega_n] \end{aligned} \quad (\text{A.20})$$

For the above three frequency conditions, the vibrating system is sometimes described as spring-controlled, damper-controlled, and mass-controlled, respectively, depending on which element is primarily responsible for the system behavior.

Curves showing the dimensionless response factor R_d as a function of the frequency ratio ω/ω_n are plotted in Fig. A.4 on the coordinate lines having a positive 45° slope. Curves of the phase angle θ are plotted in Fig. A.5. A phase angle between 180° and 360° cannot exist in this case since this would mean that the damper is furnishing energy to the system rather than dissipating it. An alternative form of A.18 and A.20 is

$$\frac{x}{F_0/k} = \frac{\left(1 - \frac{\omega^2}{\omega_n^2}\right) \sin(\omega t) - 2\zeta \left(\frac{\omega}{\omega_n}\right) \cos(\omega t)}{\left(1 - \frac{\omega^2}{\omega_n^2}\right)^2 + \left(2\zeta \frac{\omega}{\omega_n}\right)^2} = (R_d)_x \sin(\omega t) + (R_d)_R \cos(\omega t) \quad (\text{A.21})$$

This shows the components of the response which are in phase $[(R_d)_x \sin(\omega t)]$ and 90° out of phase $[(R_d)_R \cos(\omega t)]$ with the force. Curves of $(R_d)_x$ and $(R_d)_R$ are plotted as a function of the frequency ratio $\frac{\omega}{\omega_n}$ in Figs. A.6a and A.6b.

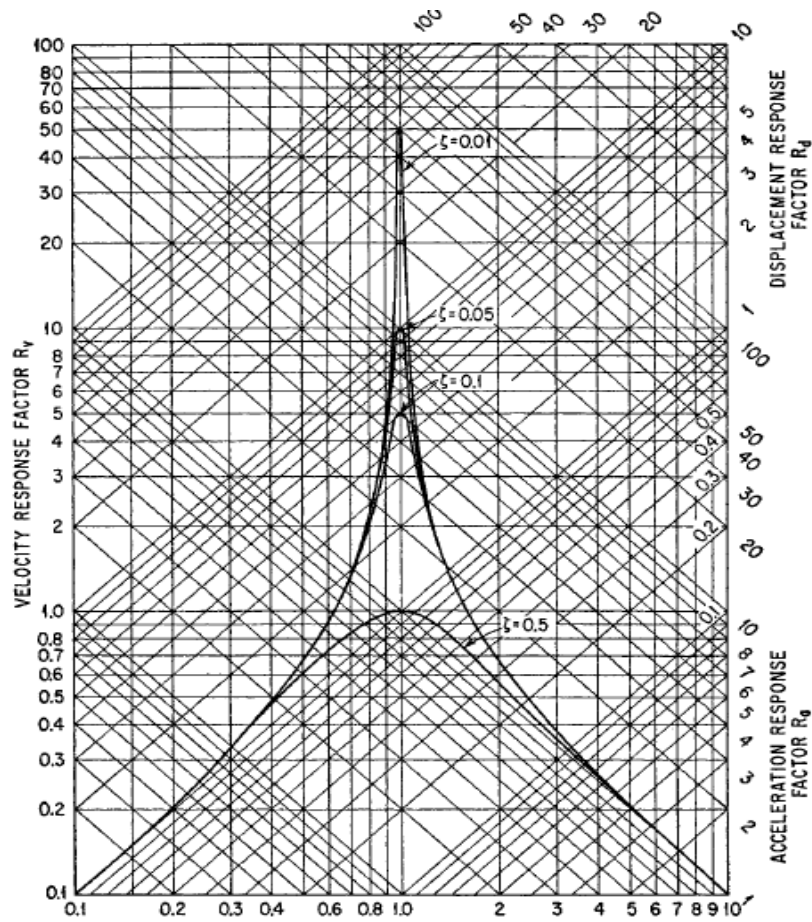


Fig. A.4. Response factors for a viscous-damped single degree-of-freedom system excited in forced vibration by a force acting on the mass. The velocity response factor is shown by horizontal lines; the displacement response factor is shown by diagonal lines of positive slope; and the acceleration response factor is shown by diagonal lines of negative slope.[2]

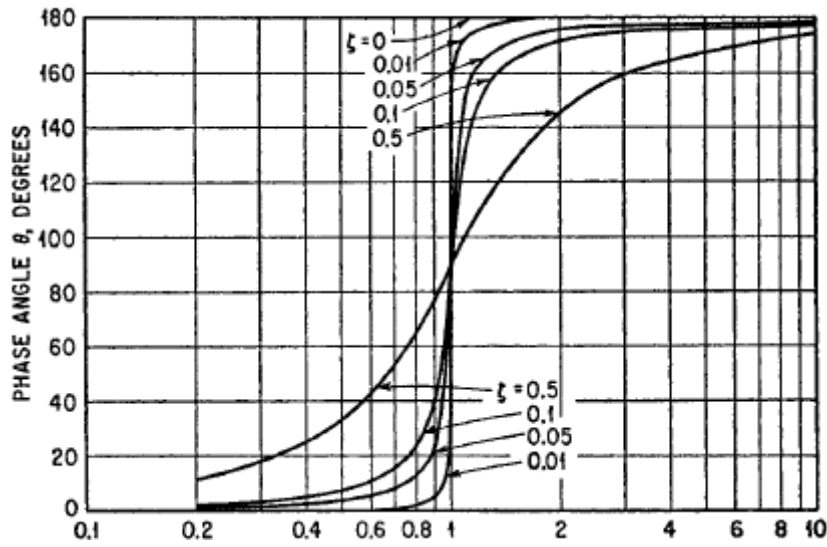
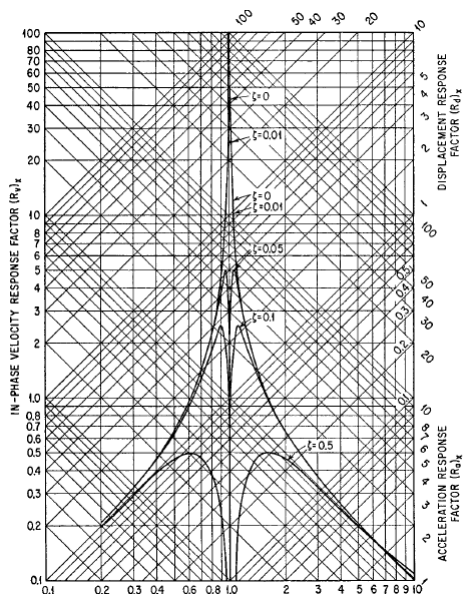
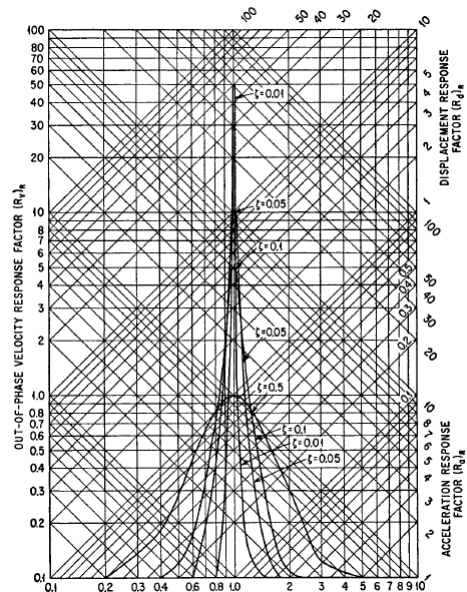


Fig. A.5. Phase angle between the response displacement and the excitation force for a single degree-of-freedom system with viscous damping, excited by a force acting on the mass of the system.[2]



(a) In-phase component of response factor of a viscous-damped system in forced vibration. All values of the response factor for $\frac{\omega}{\omega_n} > 1$ are negative but are plotted without regard for sign. The fraction of critical damping is denoted by ζ . [2]



(b) Out-of-phase component of response factor of a viscous-damped system in forced vibration. The fraction of critical damping is denoted by ζ . [2]

Fig. A.6. Response factor of a viscous-damped system

Velocity and Acceleration Response

If the graph shows velocity \dot{x} or acceleration \ddot{x} instead of displacement x the shape of the response curves changes distinctly. Differentiating A.18:

$$\frac{\dot{x}}{\frac{F_0}{\sqrt{km}}} = \frac{\omega}{\omega_n} R_d \cos(\omega t - \theta) = R_v \cos(\omega t - \theta) \quad (\text{A.22})$$

The acceleration response is obtained by differentiating A.22:

$$\frac{\ddot{x}}{\frac{F_0}{m}} = -\frac{\omega^2}{\omega_n^2} R_d \sin(\omega t - \theta) = -R_a \sin(\omega t - \theta) \quad (\text{A.23})$$

The velocity and acceleration response factors defined by A.22 and A.23 are shown graphically in Fig. A.4, the former to the horizontal coordinates and the latter to the coordinates having a negative 45° slope. Note that the velocity response factor approaches zero as $\omega \rightarrow 0$ and $\omega \rightarrow \infty$, whereas the acceleration response factor approaches 0 as $\omega \rightarrow 0$ and approaches unity as $\omega \rightarrow \infty$.

Force Transmission

The force transmitted to the foundation of the system is:

$$F_T = c\dot{x} + kx \quad (\text{A.24})$$

Since the forces $c\dot{x}$ and kx are 90° out of phase, the magnitude of the transmitted force is:

$$|F_T| = \sqrt{c^2\dot{x}^2 + k^2x^2} \quad (\text{A.25})$$

The ratio of the transmitted force F_T to the applied force F_0 can be expressed in terms of transmissibility T :

$$\frac{F_T}{F_0} = T \sin(\omega t - \Psi) \quad (\text{A.26})$$

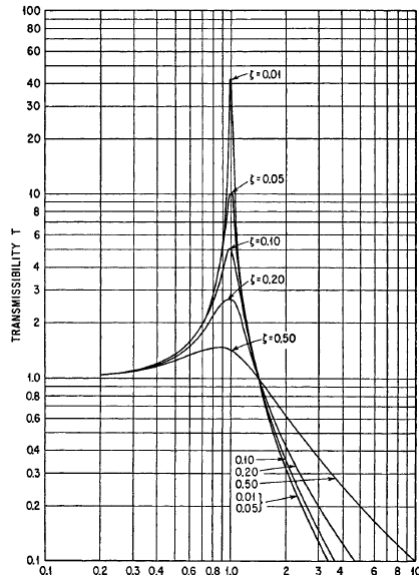
where

$$T = \sqrt{\frac{1 + \left(2\zeta \frac{\omega}{\omega_n}\right)^2}{\left(1 - \frac{\omega^2}{\omega_n^2}\right)^2 + \left(2\zeta \frac{\omega}{\omega_n}\right)^2}} \quad (\text{A.27})$$

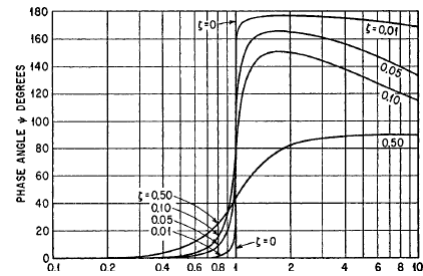
and where

$$\Psi = \tan^{-1} \frac{2\zeta \left(\frac{\omega}{\omega_n}\right)^3}{1 - \frac{\omega^2}{\omega_n^2} + 4\zeta^2 \frac{\omega^2}{\omega_n^2}} \quad (\text{A.28})$$

The transmissibility T and phase angle Ψ are shown in Fig. A.7a and Fig. A.7b, respectively, as a function of the frequency ratio $\frac{\omega}{\omega_n}$ and for several values of the fraction of critical damping ζ .



(a) Transmissibility of a viscous-damped system. Force transmissibility and motion transmissibility are identical numerically. The fraction of critical damping is denoted by ζ . [2]



(b) Phase angle of force transmission (or motion transmission) of a viscous-damped system excited by force acting on mass and by motion of foundation. The fraction of critical damping is denoted by ζ . [2]

Fig. A.7. Parameters of a viscous-damped system

Bibliography

- [1] Carlo Artero. "Topology Optimization of Aeronautical Gears". In: (2018), pp. 45–51.
- [2] Ralph E Blake. "Basic vibration theory". In: *Harris' Shock and Vibration Handbook, S* (1987), pp. 2–1.
- [3] D Nha Chu et al. "Evolutionary structural optimization for problems with stiffness constraints". In: *Finite Elements in Analysis and Design* 21.4 (1996), pp. 239–251.
- [4] Lorenzo Cucco. "Ottimizzazione topologica per componenti aeronautici realizzati in manifattura addittiva". In: (2017), pp. 68–75.
- [5] Luca D'Alò. "Multiobjective Dynamics Optimization for Aeronautical Gears". In: (2017), pp. 31–37.
- [6] Patrick Guillaume. "Modal analysis". In: *Department of Mechanical Engineering, Vrije Universiteit Brussel, Pleinlaan 2* (2007), pp. 4–6.
- [7] Ming-Hsiu Hsu and Yeh-Liang Hsu. "Generalization of two-and three-dimensional structural topology optimization". In: *Engineering optimization* 37.1 (2005), pp. 83–102.
- [8] Gupta Khurmi. *Textbook of Machine Design*. SCH, 2017.
- [9] RG Munro. "A review of the theory and measurement of gear transmission error". In: *Gearbox noise and vibration* (1990), pp. 3–10.
- [10] Erik Oberg et al. *Machinery's handbook*. Vol. 200. Industrial Press New York, 2004.
- [11] Niels Olhoff and Jianbin Du. "Topological design of continuum structures subjected to forced vibration". In: *Proc. of 6th World Congresses of Structural & Multidisciplinary Optimization (WCSMO-6)* 30 (2005).
- [12] Altair OptiStruct. "Users Guide. Altair Engineering". In: *Inc., Troy, Michigan* (2016).
- [13] R Ponginan. "Practical aspects of structural optimization". In: *A Study Guide. 2nd ed. E-book. Altair Univ* (2015).
- [14] Arash Radman. "Bi-directional evolutionary structural optimization (BESO) for topology optimization of material's microstructure". In: (2013).
- [15] Regione Piemonte. *GREAT2020*. [Online; accessed 30-September-2018]. 2012. URL: www.great2020.it/index.html.

-
- [16] Ole Sigmund and Joakim Petersson. "Numerical instabilities in topology optimization: a survey on procedures dealing with checkerboards, mesh-dependencies and local minima". In: *Structural optimization* 16.1 (1998), pp. 68–75.
- [17] Venkata Krishna Tamminana, A Kahraman, and S Vijayakar. "A study of the relationship between the dynamic factors and the dynamic transmission error of spur gear pairs". In: *Journal of Mechanical Design* 129.1 (2007), pp. 75–84.
- [18] Wikipedia contributors. *Structural Optimization/General Formulation*. 2010. URL: <http://carat.st.bv.tum.de/caratuserswiki/index.php/Users:StructuralOptimization/GeneralFormulationl>.